Global Analysis of S-nitrosylation Sites in the Wild Type (APP) Transgenic Mouse Brain-Clues for Synaptic Pathology*⒮

Monika Zaręba-Kozioł‡, Agnieszka Szwajda§, Michał Dadlez‡, Aleksandra Wysłouch-Cieszyńska‡**, and Maciej Lalowski¶‖**

Alzheimer's disease (AD) is characterized by an early synaptic loss, which strongly correlates with the severity of dementia. The pathogenesis and causes of characteristic AD symptoms are not fully understood. Defects in various cellular cascades were suggested, including the imbalance in production of reactive oxygen and nitrogen species. Alterations in S-nitrosylation of several proteins were previously demonstrated in various AD animal models and patients. In this work, using combined biotin-switch affinity/nano-LC-MS/MS and bioinformatic approaches we profiled endogenous S-nitrosylation of brain synaptosomal proteins from wild type and transgenic mice overexpressing mutated human Amyloid Precursor Protein (hAPP). Our data suggest involvement of S-nitrosylation in the regulation of 138 synaptic proteins, including MAGUK, CamkII, or synaptotagmins. Thirty-eight proteins were differentially S-nitrosylated in hAPP mice only. Ninety-five S-nitrosylated peptides were identified for the first time (40% of total, including 33 peptides exclusively in hAPP synaptosomes). We verified differential S-nitrosylation of 10 (26% of all identified) synaptosomal proteins from hAPP mice, by Western blotting with specific antibodies. Functional enrichment analysis linked S-nitrosylated proteins to various cellular pathways, including: glycolysis, gluconeogenesis, calcium homeostasis, ion, and vesicle transport, suggesting a basic role of this post-translational modification in the regulation of synapses. The linkage of SNO-proteins to axonal guidance and other processes related to APP metabolism exclusively in the hAPP brain, implicates S-nitrosylation in the pathogenesis of Alzheimer's disease. *Molecular & Cellular Proteomics 13: 10.1074/mcp.M113.036079, 2288–2305, 2014.*

The role of nitric oxide (NO)[1] as a signaling molecule in the central nervous system was discovered in 1988 (1). The brain and cerebellum in particular, contain one of the highest activities of NO-forming enzyme (NO synthase, NOS) in all tissues examined (2, 3). Nitric oxide is a freely diffusible, very reactive radical molecule. It readily reacts with various endogenous substrates forming that is, iron and copper adducts in prosthetic groups of proteins (4), peroxynitrite in the reaction with reactive oxygen species, ROS (5), and S-nitrosothiols with endogenous low-molecular weight thiols like cysteine and glutathione (6). One of the aspects of NO physiology is formation of S-nitrosylated proteins. Cysteine residues, post-translationally modified by S-nitrosylation, exert control over the activity of proteins and pathways in which they are involved, analogous to the addition of a phosphate group during phosphorylation (7, 8). S-nitrosylation is a key mechanism in the transmission of NO-based cellular signals in vital cellular processes, including: transcription regulation, DNA repair, autophagy, and apoptosis (8).

The role of protein S-nitrosylation underlying pathology of various diseases, including cancer (9, 10), heart condition

(11–13), and neurodegenerative disorders has been extensively reviewed (8, 14). In the brain, aging processes and environmental factors cause protein S-nitrosylation which in turn may enhance misfolding of proteins, induce apoptosis or autophagy, mitochondrial fragmentation and affect normal synaptic functions (8). S-nitrosylation of proteins plays an important role in neurons. For example, N-methyl-D-aspartate receptor (NMDAR) and caspase enzyme activity can be decreased by S-nitrosylation, thereby facilitating neuroprotection (15). This finding led to development of nitro-memantine, a nitric oxide donor and selective NMDAR interacting drug. It selectively S-nitrosylates the NMDA receptor and prevents its' hyperactivation, also observed in Alzheimer's disease (16). On the contrary, S-nitrosylation of protein-disulfide isomerase (17), dynamin-related protein 1 (18), glyceraldehyde dehydrogenase (19), cyclo-oxygenase-2 (20), N-ethylmaleimide sensitive protein (21), Parkin (22–24), Gospel (25), cyclin dependent kinase- 5 (26), mitochondrial complex I (27), stargazin (28), and serine racemase (29), has been related to severe neuropathological alterations in the brain caused by induction of: protein misfolding or aggregation, mitochondrial dysfunction, bioenergetic compromise, synaptic injury, and subsequent neuronal loss.

Alzheimer's disease is the most prevalent form of human dementia, with a frequency that progressively increases in aging societies (30). The temporal progression of AD exhibits a highly variable pattern among patients and is not fully understood (31). Environmental, age-related, and genetic factors have been proposed to contribute to pathogenesis of the disease. Defects in various signaling pathways regulated by post-translational modifications of proteins (PTM) that is, phosphorylation, were suggested to be the determinant parameter for disease progression (32–35). A pivotal role in development and progression of late-onset AD and various other age-dependent dementias has been attributed to inflammatory and oxidative stress cascades in the brain (36, 37). Reactive oxygen (ROS) and reactive nitrogen species (RNS) play a crucial role in these processes (38). The consequences of oxidative and nitrosative stress, such as lipid peroxidation, DNA oxidation, and nitrosative/oxidative PTM of brain proteins were detected in global and targeted proteomic analyses in AD patients (14, 39–43). On the other hand, a multitude of evidence suggests that physiological levels of ROS and RNS are implicated in various cell-signaling cascades (reviewed in (44–47)).

Various transgenic mouse models, based on the overexpression of mutant form(s) of human *APP* and recapitulating the AD phenotype are currently used to investigate mechanisms underlying disease pathology (48, 49). The present study utilized one such model, a transgenic mice expressing human *APP* with London mutation and its wild-type, aged-matched counterparts, for targeted, differential proteomic analysis of S-nitrosylation of proteins located at the synaptic terminals.

The biotin switch technique (BST) and its modification, SNOSID (SNO Site Identification) (50); in combination with mass spectrometry have been used in targeted proteomics studies of cellular "S-nitrosomes." BST relies on selective ascorbate reduction of S-nitrosothiols to generate free thiol groups in the presence of other thiol derivatives (51), whereas SNOSID (SNO Site Identification) involves biotinylation of protein SNO-Cys residues, trypsin digestion, affinity purification of biotinylated-peptides, and sequencing by tandem MS (50). The majority of such studies were undertaken to identify targets of S-nitrosylation induced by nitric oxide donor treatment (52–54).

It is however, difficult to extrapolate results of donor induced studies to an *in vivo* situation, where cysteine S-nitrosylation is dependent on the overall redox state of a cell and its unknown levels of nitrosylating compounds (55). In this work, we optimized the BST for MS-based global analysis of endogenous protein S-nitrosylation. Our study was designed to test the hypothesis that redox imbalance and changes in activity of nitric oxide synthase(s) influence the level and pattern of endogenous S-nitrosylation of synaptic proteins. Among 138 identified synaptosomal SNO-proteins, 38 were differentially S-nitrosylated in the hAPP mouse brain. Our data suggest a possibility of sequential S-nitrosylation, similarly as for other post-translational modifications, that is, phosphorylation. Focused systematic proteomics approaches addressing the role of cysteine post-translational modifications in the brain can lead to new mechanism-based therapies for various neurodegenerative disorders including AD.

EXPERIMENTAL PROCEDURES

Reagents—Bradford reagent, sucrose, Ficoll, neocuproine, and sodium ascorbate were from Sigma. S-Methyl methanethiosulfonate (MMTS) was from Fluka. Neutravidin-agarose and biotin-HPDP were purchased from Thermo Scientific. Sequencing grade modified trypsin was obtained from Promega (Madison, WI). Complete protease inhibitor mixture was from Roche diagnostics. ECL chemiluminescence reagents were purchased from Amersham Biosciences. Antibodies directed against gamma enolase (Eno2) and glial fibrillary acidic protein (Gfap) were obtained from DAKO(Carpenteria, CA). Anti-adaptor protein complex AP-2 (Ap2a1), anti-peroxiredoxin 3 (Prdx3), anti-peroxiredoxin 6 (Prdx6), and streptavidin HRP-conjugated secondary antibodies were purchased from Abcam (Cambridge, CA). Primary antibodies, directed against neural cell adhesion molecule 1 (Ncam1), synaptotagmins-1/2 (Syt1/Syt2), neurocalcin delta (Ncald), glyceraldehyde-3-phosphate dehydrogenase (Gapdh), ras-related C3 botulinum toxin substrate 1 (Rac1), inducible nitric oxide synthase 2 (Nos2; iNos), and neuronal nitric oxide synthase 1 (Nos1; nNos), as well as secondary antibodies: rabbit anti-mouse IgG, rabbit anti-goat IgG, and goat anti-rabbit IgG antibody were purchased from Santa Cruz Biotechnology. PVDF (0.22 μm) membrane was from Millipore.

Transgenic Mice—Transgenic AD mice used in this study were generated in Prof. Fred van Leuven's laboratory (K.U. Leuven) as described by Moechars *et al.* (56), and kept at the Animal House of Polish Academy of Sciences Medical Research Center. The transgenic mice express human Amyloid Precursor Protein with London mutation [Tg(APPV717I)], under the control of the mouse Thy1-gene

promoter (called later as hAPP mice). The study included 14–15 month female heterozygous mice. Control aged-matched mice (FVB/N, called later as FVB mice) were of the same genetic background. All experiments were performed in accordance with Polish guidelines for care and use of laboratory animals.

Synaptosome Isolation—Synaptosomes were prepared from brains of 14–15 months old, female FVB, and hAPP mice, as described (57, 58). Four mice of the same age were decapitated and their brains immediately removed and homogenized using Dounce homogenizer, in 6 ml of buffer A containing 5 mM Hepes pH 7.4, 0.32 M sucrose, 0.2 mM EDTA, 20 mM MMTS (a free thiol blocking reagent), and protease inhibitor mixture. The homogenate was centrifuged (2500 $\times$ g for 5 min) to yield pellet and supernatant fractions. Supernatant was subsequently centrifuged at 12,000 $\times$ g for 5 min. The obtained pellet was resuspended in buffer A, placed onto a discontinuous Ficoll gradient and centrifuged at 70,000 $\times$ g for 45 min. Synaptosomal fraction was collected, resuspended in buffer A and centrifuged at 20,000 $\times$ g for 20 min. Purified fraction of synaptosomes was used in all proteomic experiments.

Biotin Switch Technique—Substitution of S-nitrosylated Cys (SNO-Cys) sites with S-biotinylated Cys in synaptosomal protein lysates was based on a previously described BST procedure (51). In our study, we optimized concentration of used reagents and the time reactions to increase the specificity and sensitivity of the method. Mouse synaptosomal fractions were dissolved in HEN buffer containing 250 mM Hepes pH 7.7, 1 mM EDTA and 0.1 mM neocuproine. To avoid rearrangements of thiol modifying groups, the protein mixture was treated with two volumes of a thiol blocking solution containing 250 mM Hepes pH 7.7, 1 mM EDTA, 0.1 mM neocuproine (copper ion chelator), 5% SDS, and 20 mM MMTS at 50 °C for 20 min with agitation (in the dark). To remove excess of reagents, proteins were precipitated with acetone and resuspended in the same volume of HEN buffer containing 2.5% SDS. The obtained protein solutions were divided into two equal parts. One part was treated with a mixture of 400 μM Biotin-HPDP and 5 mM sodium ascorbate. The second half was used as a negative control for experiments and treated with 400 μM biotin HPDP without sodium ascorbate. All samples were incubated in the dark for 1.5 h at room temperature (RT). The proteins were again acetone-precipitated, resuspended in the same volume of HEN buffer containing 2.5% SDS and diluted with two volumes of neutralization buffer (20 mM Hepes, pH 7.7, 100 mM NaCl, and 1 mM EDTA). 100 μl of neutravidin-agarose beads was added to the solution and incubated for 1 h at room temperature with agitation. Afterward, the beads were washed five times with 20 mM Hepes, pH 7.7, 600 mM NaCl, and 1 mM EDTA and incubated with elution buffer containing 50 mM Tris, pH 8.0, 1 mM EDTA, and 50 mM DTT, for 20 min at RT with gentle agitation. The supernatants containing enriched SNO-proteins were used in subsequent Western blot analyses for validation of detected SNO-sites.

Western Blot Detection of nNos and iNos in FVB and hAPP Mouse Brains—Brain homogenates were analyzed for nNos and iNos protein expression using Western blot method. 20 μg of protein extracts from whole brains of FVB and hAPP mice, respectively, were separated by reducing 10% SDS-PAGE. Separated proteins were transferred onto PVDF membrane. The membranes were first blocked with caseine-based buffer (Sigma) and incubated with primary antibodies to nNos and iNos. Membranes were then probed with secondary antibodies raised against the appropriate species. Equal protein loads were assessed with antibodies against Gapdh and by Ponceau S staining on the blots. Western blots were developed using ECL chemiluminescence. The scanned blots were quantified densitometrically using GelQuant software and relative protein abundance of nNos and iNos normalized to the expression of Gapdh. Heteroschedastic two-tailed *t* test was used to assess the changes in expression.

Western Blot Analysis of Protein S-nitrosylation Pattern in FVB and hAPP Synaptosomes—Total synaptosomal protein fractions after BST procedure but without neutravidin-based affinity purification were resolved using reducing 10% SDS-PAGE. Selectively biotinylated proteins were captured using streptavidin-HRP conjugated antibodies and visualized by ECL chemiluminescence.

Western Blot Detection of Differential S-nitrosylation in the Brain—All fractions (including total synaptosomal fractions and those from different steps of BST procedure) were separated using 12% SDS-PAGE and transferred to PVDF membrane (0.22 μm). The membranes were first blocked with caseine-based buffer (Sigma) and incubated with primary antibodies followed by secondary HRP-conjugated antibodies. Protein bands were detected using the ECL chemiluminescence system (Amersham Biosciences). The fractions containing enriched S-nitrosylated proteins, from FVB and hAPP synaptosomes were quantified densitometrically with GelQuant software. Heteroschedastic two-tailed *t* test was used to statistically assess the changes in endogenous protein S-nitrosylation.

SNOSID—The synaptosomal protein fractions containing biotin labeled proteins (biotin labeling step described in the BST section) were digested using sequencing grade modified trypsin for 16 h at 37 °C. Digestion was terminated using protease inhibitors mixture. Tryptic peptides were incubated with 100 μl of neutravidin beads for 1 h at RT. Beads were then washed five times with 1 ml of wash buffer. Peptides bound to neutravidin resin were eluted with 150 μl of elution buffer containing 30 mM dithiotreitol. Eluted, cysteine-containing peptides were alkylated using 200 mM iodoacetamide. In the next step, peptides containing fractions were concentrated using SpeedVac and diluted with 1% trifluoroacetic acid/water (v/v) to a final concentration of 0.1% TFA.

LC-MS and LC-MS/MS Analysis—Each enriched SNO-peptides containing sample was measured twice: once with LC-MS/MS (tandem mass spectrometry), to identify the enriched SNO tryptic peptides, and once in LC-MS mode (resulting in profile spectrum), to attain label-free quantitative data based solely on peak intensities. All MS runs were separated by blank ones to reduce carry-over of peptides from previous samples. The measurements were carried in Nano Aquity Liquid Chromatography system (Waters, Milford, MA) coupled to LTQ-FTICR mass spectrometer (Thermo Scientific). SNO-peptides in 0.1% TFA were loaded from a cooled (10 °C) autosampler tray to a pre-column (Symmetry C18, 180 μm $\times$ 20 mm, and 5 μm Waters) and resolved on BEH130 column (C18, 75 μm x 250 mm, 1.7 μm, Waters), in a gradient of 5–30% acetonitrile/0.1% formic acid for 70 min at a 0.3 μl/min flow rate. The UPLC system was directly connected to the ion source of the mass spectrometer. The resolution of mass spectrometer was set to 50,000 for MS acquisitions with *m/z* measurement range of 300–2000 Th. The quantitative LC-MS runs were converted into 2D heat-maps (with retention time and *m/z* as vertical and horizontal axes, respectively) using in-house designed finnigan2Pipe data conversion tool (59, 60). The format of resulting data met the requirements of NMRPipe software (http://spin.niddk.nih.gov/NMRPipe).

For LC-MS/MS runs, we utilized the data dependent acquisition (DDA) mode, selecting the five most intense signals in each MS spectrum for fragmentation. Dynamic exclusion was activated, with m/z tolerance of 0.05–1.55 and duration of 15. Up to five fragmentation events were allowed for each parent ion. The peak-picking was performed using MascotDistiller software (version 2.3, MatrixScience, Boston, MA). Mascot search engine was used to survey data against UniProtKB/Swiss-Prot database version 2013_10 (45889 sequences). Mascot search parameters were set as follows: taxonomy *Mus musculus*, fixed modification - cysteine carbamidomethylation, variable modification - methionine oxidation, parent ion mass tolerance - 40 ppm, fragment ion mass tolerance - 0.8 Da, number of missed cleav-

ages - 1, enzyme specificity - semi-trypsin. The false-positive rate (FDR) values for Mascot identifications were calculated using the concatenated target/decoy database search strategy (merged target/decoy databases generated with *in-house* developed software (http://proteom.ibb.waw.pl/decoy/index.html). This analysis demonstrated that for peptides with Mascot score > 30, the FDR did not exceed 0.29%.

Using *in-house* developed software *Mscan* (http://proteom.ibb.waw.pl/mscan), the peptides identified in all LC-MS/MS runs (both from FVB and hAPP samples) were merged into one selected peptide list (SPL). Each peptide in the SPL was characterized by its amino acid sequence, LC retention time, *m/z* value and charge state values of corresponding ions. The SPL was then used to localize the peptide ions on 2D heat-maps generated from LC-MS runs (supplemental Fig. S1), and to obtain the quantitative values (LC peak intensities). Peptide ion localization was performed with *in-house* developed *TagProfile* software (60). Further manual data inspection (mainly to account for retention time variation in different LC runs and deal with faulty assignment cases) and quantitative analysis was achieved using *in-house* developed software *Msparky* (http://proteom.ibb.waw.pl/msparky), a modified version of Sparky NMR software (http://www.cgl.ucsf.edu/home/sparky) (59–63). Acceptance criteria for manual data inspection included: *m/z* value deviation, 20 ppm; retention time deviation, 10 min, and envelope root mean squared error (a deviation between the expected isotopic envelope of the peak heights and their experimental values) - 0.7. Charge state value was also inspected.

The SPL with obtained quantitative values was then reduced so that each cysteine was represented by single peptide entry with one quantitative value. In the final step, two lists of SNO-peptides/proteins from 14 month old mice were generated, one for hAPP and one for FVB. By comparing these lists, three sets of SNO-Cysteine peptides were determined: (1) identified only in FVB (corresponding proteins named as S-nitroso-wt), (2) identified in both FVB and hAPP (corresponding proteins named as S-nitroso-all), and (3) observed exclusively in hAPP synaptosomes (corresponding proteins named as S-nitroso-diff). These sets are presented in supplemental Table S1. The annotated spectra displaying sequence information of all identified SNO-peptides are presented in supplemental Fig. S2. All raw data from LC-MS and LC-MS/MS measurements are available at the public repository ProteomicsDB (project entitled: "synaptosomes;" https://www.proteomicsdb.org/proteomicsdb/#projects/4161?accessCode=f5247f4f64cc04f627a141ffa16b4d7d836dfabaf4c33729a990b1794723ea1b).

To compare the number of identified SNO-proteins and SNO-sites in all three sets we utilized Venny (http://bioinfogp.cnb.csic.es/tools/venny/) (64). Positions of SNO-Cys sites, the number of cysteines in protein sequence, and previously identified entries with literature references are listed in the same supplemental table. Comparison of mouse and human differential SNO-peptide sequences was achieved with Uniprot/blast program (http://www.uniprot.org/blast/).

Functional Analysis of Proteomic Data—In order to connect the human orthologs of mouse differentially S-nitrosylated gene products with Amyloid Precursor Protein (APP) we utilized *GeneMania* (www.GeneMania.org; which indexes 1464 association networks containing 292,680,904 interactions mapped to 149,747 genes from seven organisms, last update 06/2013) (65, 66). Human orthologs of mouse genes were assigned with NCBI homologene (http://www.ncbi.nlm.nih.gov/sites/homologene/). NCBI Gene unique identifiers of human orthologs of mouse genes representing differentially mouse SNO-proteins identified in FVB or hAPP mice were used as an input for functional network analyses. The networks were calculated and drawn using *GeneMania* reference real- and binary-valued interaction networks consisting of physical, genetic, predicted, and pathway interaction data sets. For weighting of the networks we used Gene
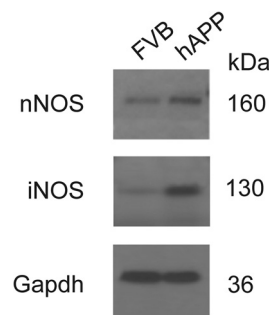

FIG. 1. **Western blot analysis of iNOS and nNOS expression in the brain.** The expression of both enzymes was analyzed in wild-type (FVB, lane 1) and transgenic APP (hAPP, lane 2) total mouse brain cortex lysates. Gapdh protein expression was used for normalization. kDa- molecular weight in kilo-Daltons.

Ontology biological process (GO BP) algorithm from *GeneMania*, which assigns weights in order to maximize connectivity between all input genes in a given ontology class. The number of measured SNO-sites was included as one of the parameters in network depiction. In cases when the number of SNO-sites in a peptide after neutravidin affinity could not be unambiguously assigned, for simplicity, we chose the highest possible number of SNO-sites, according to a number of available Cys in a given sequence.

SNO-data sets were functionally analyzed using ClueGOv1.4, a Cytoscape plug-in (http://www.ici.upmc.fr/cluego/) (67), which applies GO/KEGG hierarchical characteristics for clustering of term distributions. As a reference set for term enrichment calculations we utilized genes (NCBI unique Gene identifiers), corresponding to human orthologs of MS- measured mouse synaptosomal proteins (Malinowska *et al.*, submitted), enriched with non-redundant genes from two most comprehensive, expert- curated synaptic databases (SynsysNet; http://bioinformatics.charite.de/synsys/ (68) and SynaptomeDB; http://psychiatry.igm.jhmi.edu/SynaptomeDB/ (69)). Thus constructed "synaptic reference set" comprises of more than 5600 NCBI unique human genes. The enrichment of GO biological process functional categories in this reference set is presented in supplemental Fig. S3. A Venn diagram demonstrating the distribution of genes among three database sources in "synaptic reference set" is presented in supplemental Fig. S4. *p* values for term enrichment were calculated using right-sided hypergeometric test. The nodes in functionally grouped networks were linked based on their kappa score level (≥0.3) in ClueGO.

RESULTS

The Protein Expression of Nitric Oxide Synthases is Elevated in hAPP Mouse Brain—Expression levels of nNOS and iNOS in total brain cortex lysates from 14 months old FVB and hAPP mice were compared by Western blot analysis. A significant increase in the protein expression levels of iNOS (fold change = 4.94, *n* = 4, *p* = 4.74E-06), and nNOS (fold change = 2.05, *n* = 2) was observed in hAPP mouse brain in comparison to FVB mouse brain, consistent with previous observations (70, 71). Bands of 130 and 160 kDa corresponded to iNOS and nNOS, respectively (Fig. 1).

Endogenous Protein S-nitrosylation is Increased in hAPP Synaptosomes—To assess whether the increased expression of nitric oxide synthases visible in the hAPP mouse brain results in pattern changes of endogenous protein S-nitrosy-
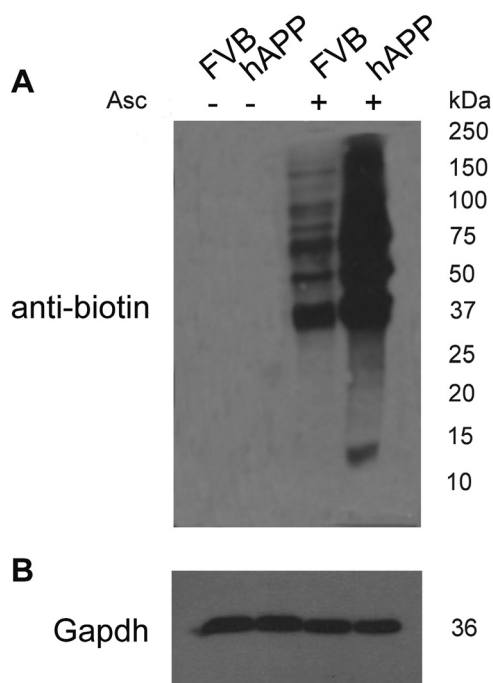
A

Asc   −   −   +   +   kDa

anti-biotin

250
150
100
75
50
37
25
20
15
10

B

Gapdh   36

FIG. 2. **Western blot analysis of S-nitrosylation pattern in the FVB and hAPP brains.** S-nitrosylation sites were selectively labeled with S-S-biotin (BST). Visualization of biotinylated proteins was achieved with anti-biotin antibodies. Controls were prepared without selective ascorbate (Asc) reduction of SNO bonds (lane 1 and 2). Pattern of S-nitrosylation of synaptosomal proteins from FVB and hAPP mouse brain is presented in lanes 3 and 4, respectively.

lation, we used a BST assay in which SNO-proteins are selectively labeled by biotin, followed by Western blot detection with anti-biotin antibodies. Numerous protein bands across a broad mass range were revealed, both in FVB and hAPP derived synaptosomal fractions indicating the presence of endogenously S-nitrosylated proteins (Fig. 2, lane 3 and 4). The number and intensities of specific bands were significantly increased in hAPP synaptosomes. No bands were detected in negative control experiments confirming selectivity of the ascorbate reduction of SNO-bonds.

Endogenously S-nitrosylated Proteins in FVB and hAPP Synaptosomes were Identified using SNOSID-LC-MS/MS Assay—BST and anti-biotin Western blot analysis suggested that synaptosomal proteins of a wide molecular mass range are affected by S-nitrosylation.

In our work, we utilized SNOSID technique developed by Hao *et al.* (50) for non- targeted proteomic identification of specific cysteine residues in proteins which are modified by posttranslational S-nitrosylation. The method is based on exclusive affinity capture of formerly nitrosylated, cysteine containing tryptic peptides, which are labeled with biotin similarly as in the initial steps of BST assay. The overall scheme of S-nitrosylation enrichment methodology used in this work is presented in the Fig. 3.

We explored SNOSID peptide enrichment technique combined with LC-MS/MS peptide identification to precisely as-

certain the targets of S-nitrosylation among synaptosomal proteins. Among 138 identified SNO-proteins, 38 were present only in hAPP mice synaptosomes (Fig. 4A, Table I and supplemental Table S2). A total of 249 SNO-sites were identified, including 108 sites found exclusively in hAPP brain (Fig. 4B). Sequence alignment of mouse differentially S-nitrosylated peptide sequences with their human counterparts demonstrated that almost all SNO- Cys are conserved between both species (supplemental Table S3). 95 SNO- peptides were identified for the first time (40% of total, 33 of which were solely present in hAPP synaptosomes). 49 of the hAPP differential SNO-sites were detected in proteins S-nitrosylated in FVB mice but at a different Cys residue, that is, in calcium/calmodulin-dependent protein kinase II (CamkII), succinate-CoA ligase (Suclg1), or neurofascin (Nfasc). Interestingly, for aconitate hydratase (Aco2) we detected an exchange of a single SNO-site from Cys385 to Cys592. The number of differential SNO-peptides, that is, SNO-sites in FVB and hAPP mice differs from that of differential proteins, which suggests that some proteins are possibly sequentially S-nitrosylated.

The overall pattern of S-nitrosylations in FVB and hAPP synaptosomes is depicted in supplemental Fig. S5. Fig. 4C schematically portrays the possibilities for SNO-based regulation of synaptosomal proteins as a result of the hAPP overexpression in mice.

Synaptosomal S-nitrosylated Proteins in FVB Mouse Brain Represent a Variety of Protein Classes—In order to decipher molecular mechanisms in the synapse, in which S-nitrosylation of proteins might play a distinct role, we performed functional enrichment analyses of terms from Gene Ontology Biological Process (GOBP) and KEGG. For this purpose, we utilized a comprehensive "synaptic reference set," comprising over 5600 genes (see description in Material and Methods) and ClueGO algorithm. Two sets of identified human orthologs of mouse S-nitrosylated synaptosomal proteins (S-nitroso-wt and S-nitroso-diff sets) were analyzed. The analyses of S-nitroso-wt set (Fig. 5 and supplemental Tables S4) revealed multiple enriched functional categories. Terms related to: generation of precursor metabolites ($p = 3.11E-15$), gluconeogenesis ($p = 7.41E-08$), synaptic transmission ($p = 1.22E-4$), and neurotransmitter transport ($p = 1.07E-03$) were significantly statistically enriched in GO BP analyses of S-nitroso-wt set (Fig. 5 and supplemental Table S4A). In-depth analysis of KEGG pathways pinned down additional enriched terms related to other metabolic processes, that is, TCA cycle, oxidative phosphorylation and synaptic organization, to name but only a few of those most associated with the normal physiology of neurons.

The multiplicity of enriched terms suggests that S-nitrosylation is a global post-translational modification, with a role in modulating the function of different classes of proteins within the synapse microenvironment. Interestingly, 16 SNO-proteins from FVB mice (~12% of all identified mouse brain
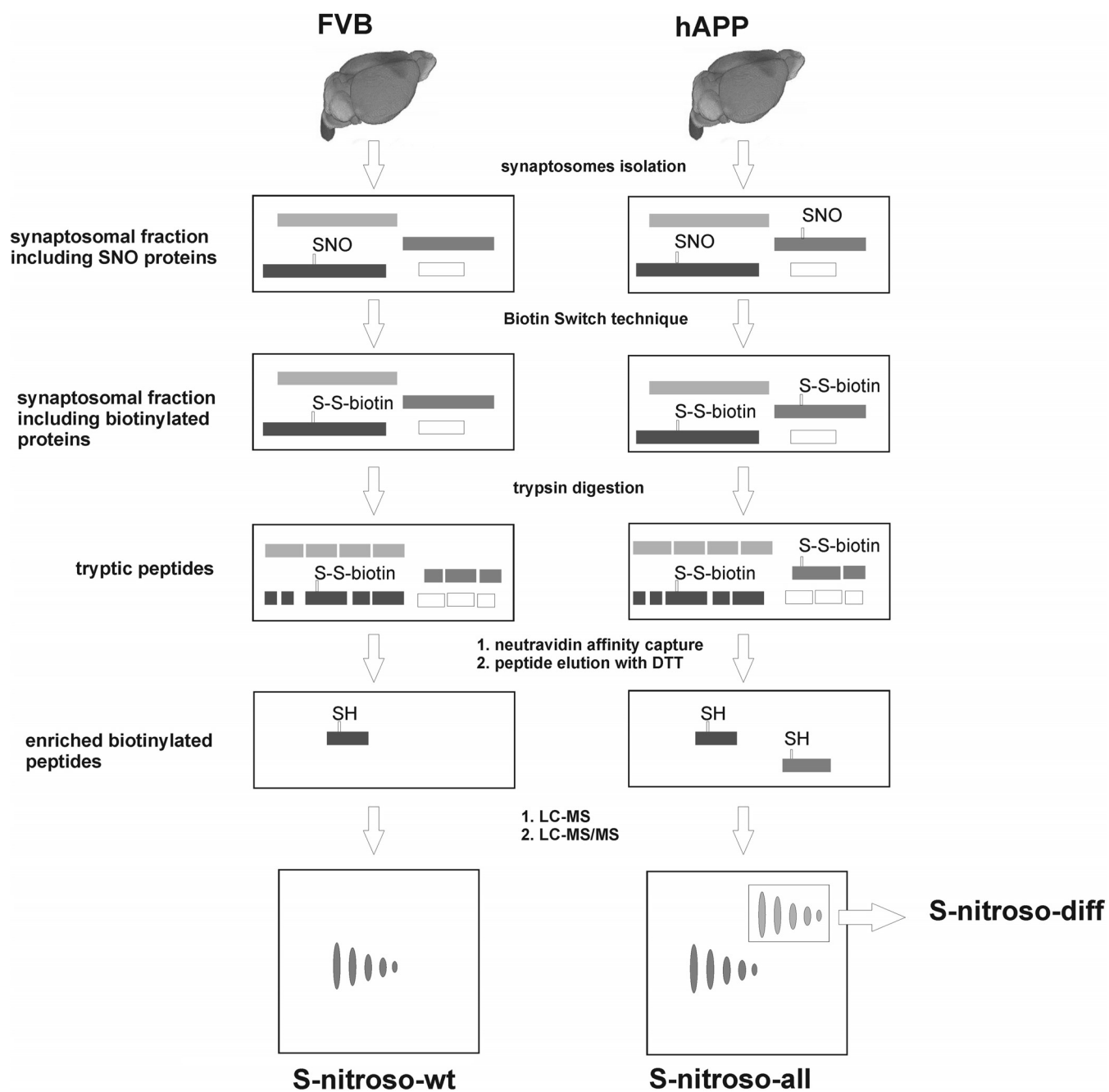
FIG. 3. **Scheme of S-nitrosylation enrichment methodology.** Mouse brain synaptosomes were isolated and S-nitrosylated proteins enriched using Biotin Switch Technique. After trypsin digestion and enrichment on Neutravidin agarose, the SNO-peptides were analyzed by LC-MS/MS using *in house* developed *MSparky* software.

synaptosomal SNO-proteins; supplemental Table S4B) formed a cluster of functionally grouped terms (Fig. 5) previously implicated in Alzheimer's, Parkinson's, and Huntington's diseases.

Differentially S-nitrosylated Proteins in hAPP Mouse Brain are Linked to Axon Guidance and Vesicle Trafficking and Form a Highly Connected Network—Analysis of S-nitroso-diff proteins with ClueGO and GO BP revealed two major functional clusters. Similarly, as in the wild-type mouse brain, a six node

subnetwork related to gluconeogenesis/glycolysis and generation of precursor metabolites and energy was revealed (comprising nine out of 38 analyzed proteins, supplemental Table S5A). The second subnetwork contained 11 nodes including axon guidance (GO:0007411), which presented the most enriched group term ($p = 4.76E-03$; Fig. 6A, 6B). Other nodes which belong to this functional cluster included that is, vesicle mediated transport and exocytosis, both of which are linked to APP neuronal trafficking (Fig. 6B and supplemental Table S5B)

FIG. 4. **Venn diagram comparisons of the numbers of S-nitrosylated proteins A, and S-nitrosylation sites B,** identified in synaptosomes isolated from FVB and hAPP mouse brains. *C,* Scheme of S-nitrosylation pattern in S-nitroso-wt and S-nitroso-all sets showing differential and sequential S-nitrosylation, respectively. The details on number of SNO-Cys and SNO-sites identified in this study with respective UniProtKB/Swiss-Prot IDs and NCBI Gene Symbols are given in supplemental Fig. S5.
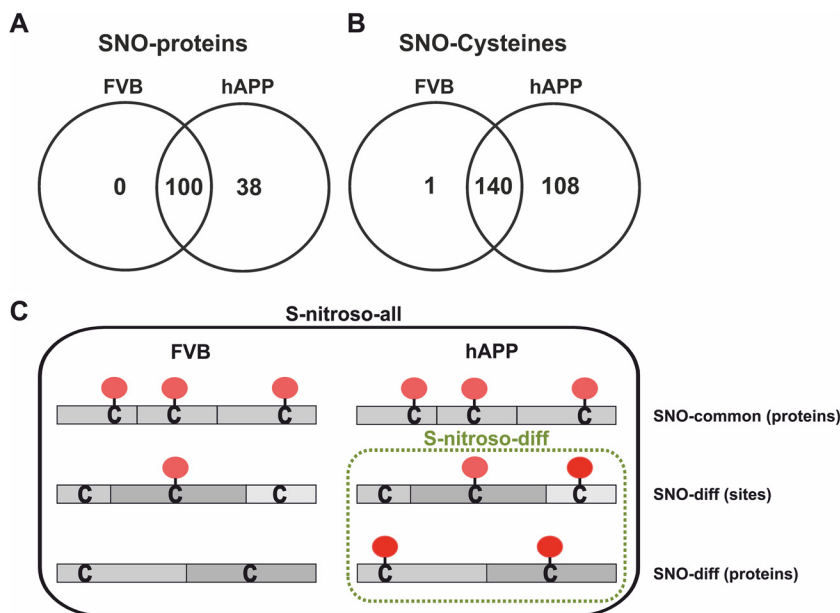
(72, 73). Parallel functional analyses using KEGG pathways supported the finding that proteins in the S-nitroso-diff set are linked to axon guidance and regulation of actin cytoskeleton ($p = 3.71E-02$, Fig. 6B and supplemental Table S5B).

In this study, human APP protein expression in mouse brain was the distinguishing parameter used to model some aspects of Alzheimer disease. Therefore, we aimed to assess the connectivity of the identified differentially S-nitrosylated synaptosomal proteins to APP. We searched for human orthologs of mouse SNO-proteins (supplemental Table S1) and connected them using Gene*Mania*. We connected 36 (out of 38) differentially S-nitrosylated orthologs with APP using multiple interaction data (Fig. 6C and supplemental Tables S6A–S6D). Fifty-nine nodes in the calculated network (supplemental Table S6A) were connected by genetic (57 links) and physical interactions (34 links), as well as pathway sharing (27 links). Thirty-four interactions in the network were derived from predicted, mostly interologous interactions (supplemental Table S6B). Five SNO-proteins were directly connected to APP either via physical interactions (Gapdh/GAPDH), genetic interactions (Ube2d3/UBE2D3, Negr1/NEGR1), and pathway sharing (Gapdh/GAPDH and Negr1/NEGR1) or predicted to interact from homologous interactions (Ncam1/NCAM1). Actb/ACTB (β-actin) has been detected as part of the same molecular complex with APP (74). The most enriched functional category of the network, participation in cytoplasmic vesicle ($p = 2.74E-04$) was shared by nine proteins, including APP and 6 SNO-proteins, namely AP2A1, ALDOA, HSPA8, NCALD, SYT1, and SYT2. Subsequent analysis of the axon guidance subnetwork ($p = 1.73E-03$) revealed that it contained 10 proteins, including APP, PRNP, LIMK1, and AGRN and six human orthologs of differentially nitrosylated proteins (from S-nitroso-diff set): ACTB, AP2A1, CFL1, KRAS, NCAM1, and RAC1 (Fig. 6C and supplemental Table S6C).

*Validation of Differential Protein S-nitrosylation Detected using Biotin Switch-LC-MS/MS by Western Blotting—*Western blot analysis was used to validate the results of MS based identifications of selected, differential SNO-proteins implicated in AD (75–79). Immunoreactivity was traced in different fractions during BST enrichment of S-nitrosylated synaptosomal proteins from FVB and hAPP mice. Ten differentially S-nitrosylated proteins from different functional classes were chosen for MS data validation (including a novel one described in this study, neurocalcin delta, Ncald). Fig. 7 demonstrates the results of immunoblotting with specific antibodies recognizing mouse Ncam1, Ap2a1, Gfap, Eno2, Syt1/Syt2, Gapdh, Ncald, Prdx3, and Rac1, respectively. The total expression of studied proteins was unchanged in the hAPP and FVB brains (lanes 1 and 2), which is consistent with the results of differential proteomics expression analysis in these mice (Malinowska *et al.*, submitted). Following BST enrichment, positive signals were observed only in fractions derived from hAPP brain synaptosomes (lane 7), but not in the FVB brain (lane 5), confirming the MS-based identification of differentially SNO-proteins. An internal control in which S-nitrosylation does not change between FVB and hAPP (includes two synaptosomal proteins, synaptophysin, Syp, and peroxiredoxin, Prdx6; compare lanes 5 and 7, Fig. 7A, 7B) was included.

Interestingly, a specific monoclonal antibody against enolase 2, Eno2 was used to positively identify S-nitrosylation of this protein in the hAPP brain. In MS based analyses we could not distinguish whether this protein is differentially S-nitrosylated in hAPP mice or an additional site is modified by S-nitrosylation upon APP overexpression (supplemental Table S2A). The identified SNO-peptide in the FVB synaptosomes was also shared between three enolases, Eno1, Eno2, and Eno3, precluding a proper assignment. The results of Western

TABLE I

List of identified, differentially S-nitrosylated proteins and corresponding peptides in the synaptosomes from hAPP transgenic mice. Legend: Name, UniProtKB/Swiss-Prot name, ID, UniProtKB/Swiss-Prot database unique identifier; Gene Symbol, NCBI official Gene Symbol, Mus Musculus; Peptide sequence, sequence of the Cys containing peptide identified in our MS/MS experiments; SNO-peptide, SNO-peptides detected in MS/MS measurements; Cys, number of Cysteines in a given protein sequence; #, literature described endogenous S-nitrosylation of Cys from a given peptide sequence; *, literature described exogenous S-nitrosylation of Cys from a given peptide sequence. Ref, Literature citation (see references). All Cys in the sequence are bold marked. Differentially SNO-Cysteines are marked in red. The aminoacid position of Cys-SNO is given in subscript. In cases where SNO modification could not be unambiguously assigned (i.e. 2v3), the potentially SNO-Cys (in bold red) are underlined. Ref- cited literature

Name	ID	Gene Symbol	Peptide sequence	SNO-pept	SNO-Cys	Cys	Ref
Acylphosphatase-2	P56375#	Acyp2	SVDYEVFGTVQGVC_{30}FR #	+	1	1	(107)
Glial fibrillary acidic protein	P03995*	Gfap	QLQALTC_{291}DLESLR	+	1	1	(92, 137)
Neurocalcin-delta	Q91X97	Ncald	LLQC_{185}DPSSAGQF	+	1	2	
40S ribosomal protein S11	P62281#	Rps11	C_{60}PFTGNVSIR #	+	1	3	(107)
Heat shock cognate 71 kDa protein	P63017#*	Hspa8	GPAVGIDLGTTYSC_{17}VGVFQHGK	+	1	4	(53, 92, 107, 138-140)
Ubiquitin-conjugating enzyme E2 D3	P61079#	Ube2d3	IYHPNINSNGSIC_{85}LDILR #	+	1	4	
Cofilin-1	P18760#	Cfl1	AVLFC_{39}LSEDKK #	+	1	4	(107, 141)
Thioredoxin-dependent peroxide reductase, mitochondrial	P20108#	Prdx3	AFQFVETHGEVC_{230}PANWTPESPTIKPSPTASK #	+	1	4	(107)
MAGUK p55 subfamily member 2	Q9WV34#	Mpp2	DLELTPTSGTLC_{310}GSLSGK #	+	1	5	(50, 142)
GTPase KRas	P32883	Kras	TGEGFLC_{80}VFAINNTK	+	1	5	
Methylglutaconyl-CoA hydratase, mitochondrial	Q9JLZ3#	Auh	SEVPGIFC_{113}AGADLK #	+	1	5	(107)
Synaptotagmin-1	P46096*	Syt1	LGDIC_{277}FSLR	+	1	6	(139)
Acetyl-CoA acetyltransferase, mitochondrial	Q8QZT1#*	Acat1	QATLGAGLPISTPC_{116}TTVNK *#	+	1	6	(107, 138)
Fructose-bisphosphate aldolase C	P05063#	Aldoc	C_{290}PLPRPWALTFSYGR #	+	1	7	(92, 107, 139)
Synaptotagmin-2	P46097#	Syt2	LTVC_{293}ILEAK #	+	1	9	(142)
P2X purinoceptor 6	O54803	P2rx6	LC_{347}DLLLLYVDR	+	1	13	
Choline transporter-like protein 2	Q8BY89	Slc44a2	VVDDTAC_{401}PLLR	+	1	26	
Neuronal growth regulator 1	Q80Z24	Negr1	DYSLQIQNVDVTDDGPYTC_{112}SVQTQHTPR	+	1	12	
LanC-like protein 2	Q9JJK2	Lancl2	TIVC_{187}QESELPDELLYGR	+	1	13	
Ly-6/neurotoxin-like protein 1	Q9WVC2	Lynx1	KSC_{64}VPSC_{68}FETVYDGYSK	+	1v2	10	
Metallothionein-1	P02802#*	Mt1	S$\underline{C_{33}}\underline{C_{34}}S\underline{C_{36}}\underline{C_{37}}PVG\underline{C_{41}}$SK *#	+	1v2v3 v4v5	20	(107)
Creatine kinase B-type	Q04447#*	Ckb	FC_{254}TGLTQIETLFK	+	2	5	(53, 139, 141)
			LGYILTC_{283}PSNLGTGLR *#	+			
Vacuolar ATP synthase subunit B, brain isoform	P62814#	Atp6v1b2	KTSC_{112}EFTGDILR	+	2	6	(50, 142)
			LALTTAEFLAYQC_{289}EK	+			
Actin, cytoplasmic 1	P60710#*	Actb	LC_{217}YVALDFEQEMATAASSSSLEK #	+	2	6	(53, 92, 107, 138, 139, 141, 143)
			C_{285}DVDIR #	+			
Myelin-oligodendrocyte glycoprotein	Q61885	Mog	ALVGDEAELPC_{52}R	+	2	7	
			FSDEGGYTC_{126}FFR	+			
Sodium/potassium-transporting ATPase subunit beta-2	P14231	Atp1b2	SC_{10}GQVVEEWKEFVWNPR	+	2	7	
			NDVC_{129}RPGR	+			
			ALANSLAC_{338}QGK *#	+			
Neural cell adhesion molecule 1, 180 kDa isoform precursor	P13595*	Ncam1	FFLC_{41}QVAGDAK	+	2	14	(139)
			NAPTPQEFKEGEDAVIVC_{139}DVVSSLPPTIIWK	+			
Elongation factor 2	P58252#*	Eef2	STLTDSLVC_{41}K #	+	2	17	(107, 138, 141)
			ETVSEESNVLC_{591}LSK *#	+			
Sarcoplasmic/endoplasmic reticulum calcium ATPase 2	O55143#*	Atp2a2	VGEATETALTC_{447}LVEK *#	+	2	29	(107, 138)
			NYLEQPGKEC_{998}VQPATK #	+			

TABLE I—*continued*

Protein	Accession	Gene	Peptide		Ratio	Sites	Refs
Fructose-bisphosphate aldolase A	P05064*#	**Aldoa**	YASIC$_{178}$QQNGIVPIVEP EILPDGDHDLKR #	+	2	8	(92, 107, 139)
			ALANSLAC$_{339}$QGK *#	+			
Hexokinase-1	P17710*#	**Hk1**	QTSLDC$_{669}$GILITWTK	+	2	23	(107)
			C$_{942}$TVSFLLSEDGSGK #	+			
Glyceraldehyde-3-phosphate dehydrogenase	P16858#*	**Gapdh**	IVSNSC$_{150}$TTNC$_{154}$LAPL AK *#	+	2v3	5	(92, 107, 138, 143, 144)
			VPTPNVSVVDLTC$_{245}$R *#	+			
ADP/ATP translocase 1	P48962*#	**Slc25a4**	EFNGLGDC$_{160}$LTK *#	+	3	4	(107)
			YFAGNLASGGAAGATS LC$_{129}$FVYPLDFAR #	+			
			GADIMYTGTLDC$_{257}$WR *#	+			
Triosephosphate isomerase	P17751#*	**Tpi1**	IAVAAQNC$_{117}$YK *#	+	3	6	(92, 107, 138, 143, 144)
			VSHALAEGLGVIAC$_{177}$I GEK #	+			
			IIYGGSVTGATC$_{268}$K *#	+			
Ras-related C3 botulinum toxin substrate 1	P63001#	**Rac1**	HHC$_{105}$PNTPIILVGTK #	+	3	7	(107)
			YLEC$_{157}$SALTQR #	+			
			AVLC$_{178}$PPPVK #	+			
AP-2 complex subunit alpha-1	P17426#	**Ap2a1**	ALQVGC$_{941}$LLR #	+	3	19	(107)
			LVEC$_{283}$LETVLNK	+			
			HLC$_{970}$ELLAQQF	+			
2',3'-cyclic nucleotide 3' phosphodiesterase	P16330#	**Cnp**	LDCAQLKEKPELQFPF LQDEDTVATLHEC$_{49}$K	+	4	7	(145)
			LDEDLAGYC$_{111}$R #	+			
			LDC$_{157}$AQLK	+			
			AHVTLGC$_{334}$AADVQPV QTGLDLLDILQQVK	+			
NADH dehydrogenase [ubiquinone] flavoprotein 1, mitochondrial	Q91YT0*#	**Ndufv1**	NAC$_{187}$GSDYDFDVFVV R #	+	3v4	12	(107)
			GAGAYIC$_{206}$GEETALIE SIEGK #				
			LKPPFPADVGVFGC$_{238}$ PTTVANVETVAVSPTIC$_{255}$R #				

blot analysis indicate that there is no S-nitrosylation of Eno2 in the wild-type mouse brain. Overall, we have validated the differential SNO of 10 proteins in hAPP synaptosomes.

DISCUSSION

Signaling by RNS is mainly carried out by targeted modifications of critical cysteine residues in proteins, including S-nitrosylation, S-oxidation, and lipid nitration (80). Despite thousands of SNO-proteins currently identified (~3000), the observed specificity of *S*-nitrosylation in terms of target proteins and specific Cys residues is not entirely understood (81, 82). S-nitrosylated proteins are implicated in the pathogenesis of various neurodegenerative diseases, including Alzheimer's, Parkinson's and Huntington's diseases, amyotrophic lateral sclerosis, Friedreich ataxia, and many others, where they influence the onset or development of neurodegeneration (8, 23, 83–85).

One of the key pathological features of patients with neurodegenerative disorders including AD is impaired signaling at the synapse. Our proteomics study was designed to search for and identify endogenous regulation of synaptic proteins by S-nitrosylation. We also probed for a direct association of protein S-nitrosylation with an important aspect of AD development, namely overexpression of Aβ.

Synaptosomes are a well-recognized model for studies of synaptic complexity in the brain (86, 87). They contain complete presynaptic terminals, with postsynaptic membranes and densities, as well as other components necessary to store, release, and retain neurotransmitters. Viable mitochondria for production of ATP and active energy metabolism, are also present in synaptosomes (88). Moreover, it has recently been proposed that S-nitrosylation is effectively dependent on the subcellular localization of proteins, with short-range linkage to synaptic transmission in neurons (89). Therefore, in order to reduce the complexity of the analyzed system we decided to narrow our studies to proteins involved in synaptic functions, employing fresh synaptosomal preparations routinely used for proteomic screening of affected pathways in the brain (90, 91).

A combination of different approaches based on BST and immunoprecipitation with S-nitrosothiol antibodies, followed by 2D-electrophoresis and LC-MS/MS was recently introduced by Zahid *et al.* (92), to study differentially S-nitrosylated proteins in the human AD brain. However, in their study, total brain lysates from cortex, hippocampus, and substantia nigra (*post-mortem* frozen brain tissue) were utilized, and only 45 SNO-proteins identified (without recognizing sites of modification), impeding detailed analysis of the affected pathways in the synapse.

Human brain tissue samples are difficult targets for differential proteomics. Samples are obtained *post morte*m with usually longer interval times in comparison to the life-span of most SNO-proteins. Special autopsy programs for AD pa-
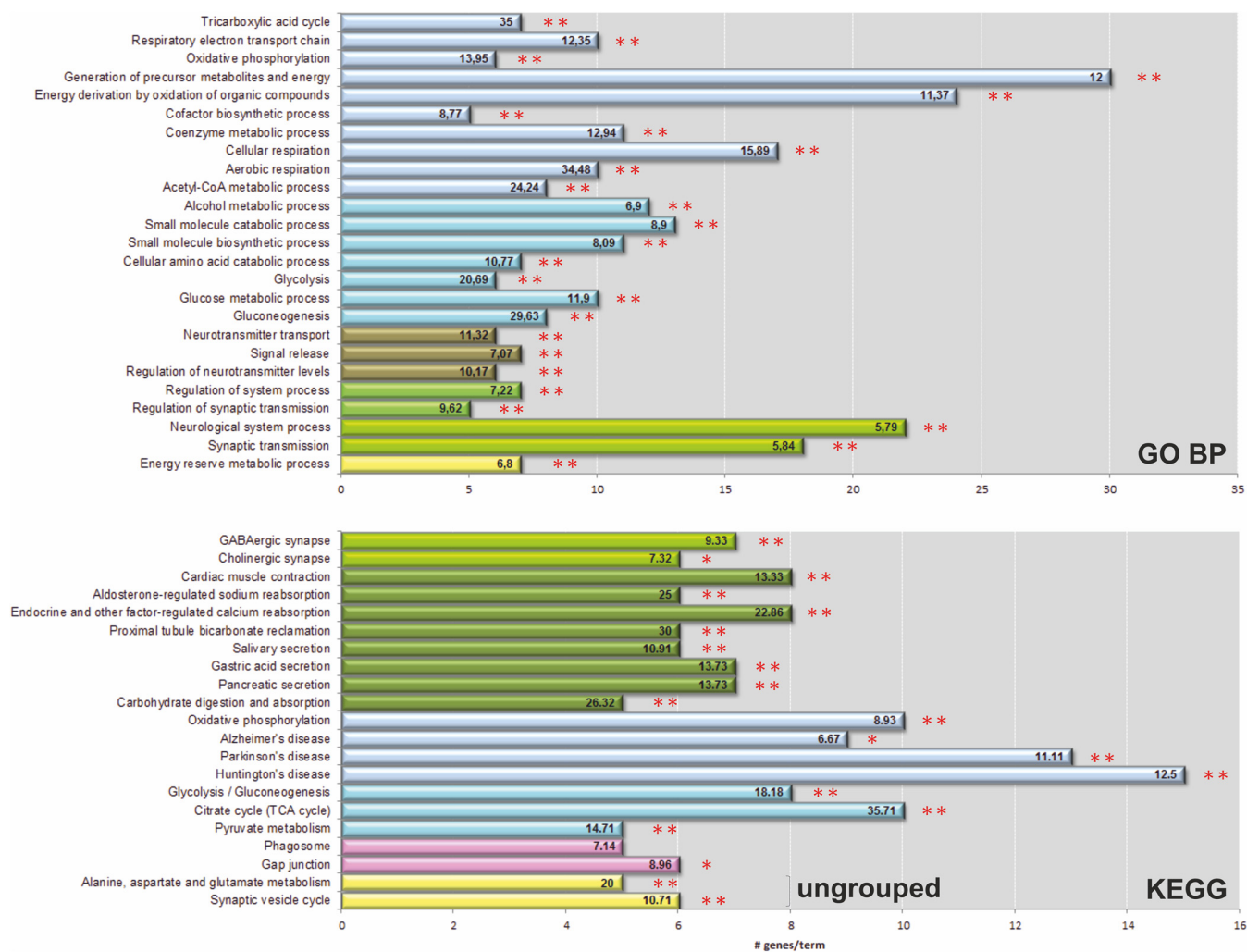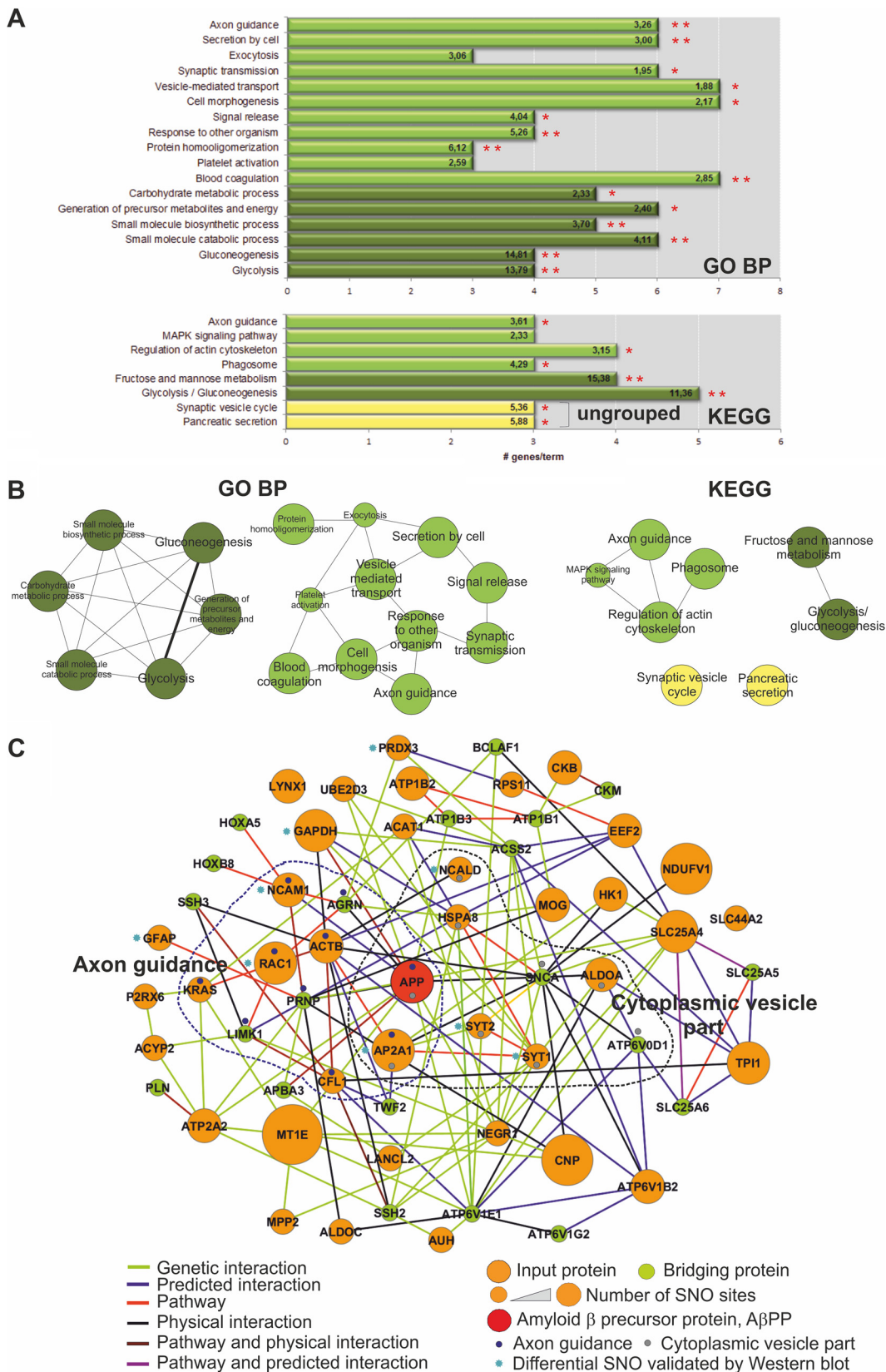
FIG. 5. **ClueGO analysis of S-nitrosylated proteins from FVB mouse brain synaptosomes.** GO biological process (GO BP, upper panel) and KEGG pathway (KEGG, lower panel) terms specific for S-nitrosylated proteins from the FVB brain synaptosomes (**-$p \leq 0.01$, *-$p \leq 0.05$). The number of corresponding genes associated with a specific term is indicated. The percentage of genes associated with a specific term is listed on the bars. Ungrouped terms are shown in yellow.

tients, aimed at analysis of labile PTM within 4-h post mortem interval are still rare (*i.e.* Rapid Autopsy Program of the University of Kentucky Alzheimer's Diseases Research Center, UKADRC (93)). Moreover, freezing and thawing of tissues leads to artifacts in tyrosine nitration and cysteine nitrosylation if homogenization is not performed in the presence of thiol blocking agents (94). As such, instead of analyzing highly variable human tissue samples (vide *i.e.* SNO Drp1 level analysis in AD patients (95)) we opted for a well-defined tg AD mouse model for differential analysis of synaptic SNO-proteins. Moreover, the inclusion criteria used for selection of differential protein sets proposed in our work were very stringent. A protein has been defined as differentially S-nitrosylated only if it was repeatedly observed in hAPP brain synaptosomes, and not detected in the age-matched wild-type controls. In the authors opinion, this led to highly selective identification of differentially SNO synaptic proteins in the hAPP brain.

Despite its utility in identifying SNO-Cys modification in proteins, the BST and SNOSID methods are constrained by several limitations. Each step of these techniques is a potential source of methodological errors. One of such limitations is linearity (with respect to protein input and biotinylation). The blocking step of the BST shall also be taken into consideration, as some protein thiols can be resistant to complete blocking, resulting in high levels of SNO-independent biotinylation. Another question which was raised by some authors is the specificity of the method. The other constraint is a usage of ascorbate, which was suggested to have a potential to reduce the disulfide bonds. This has been later challenged by observations that thiol-dependent reduction of dehydroascorbate to ascorbate, a scenario supported by extensive *in vitro* and *in vivo* experimentation is thermodynamically favored. Another limitation of BST method is related to the presence of metal ions, which can compromise the BST specificity, including production of ascorbate and hydroxyl radi-
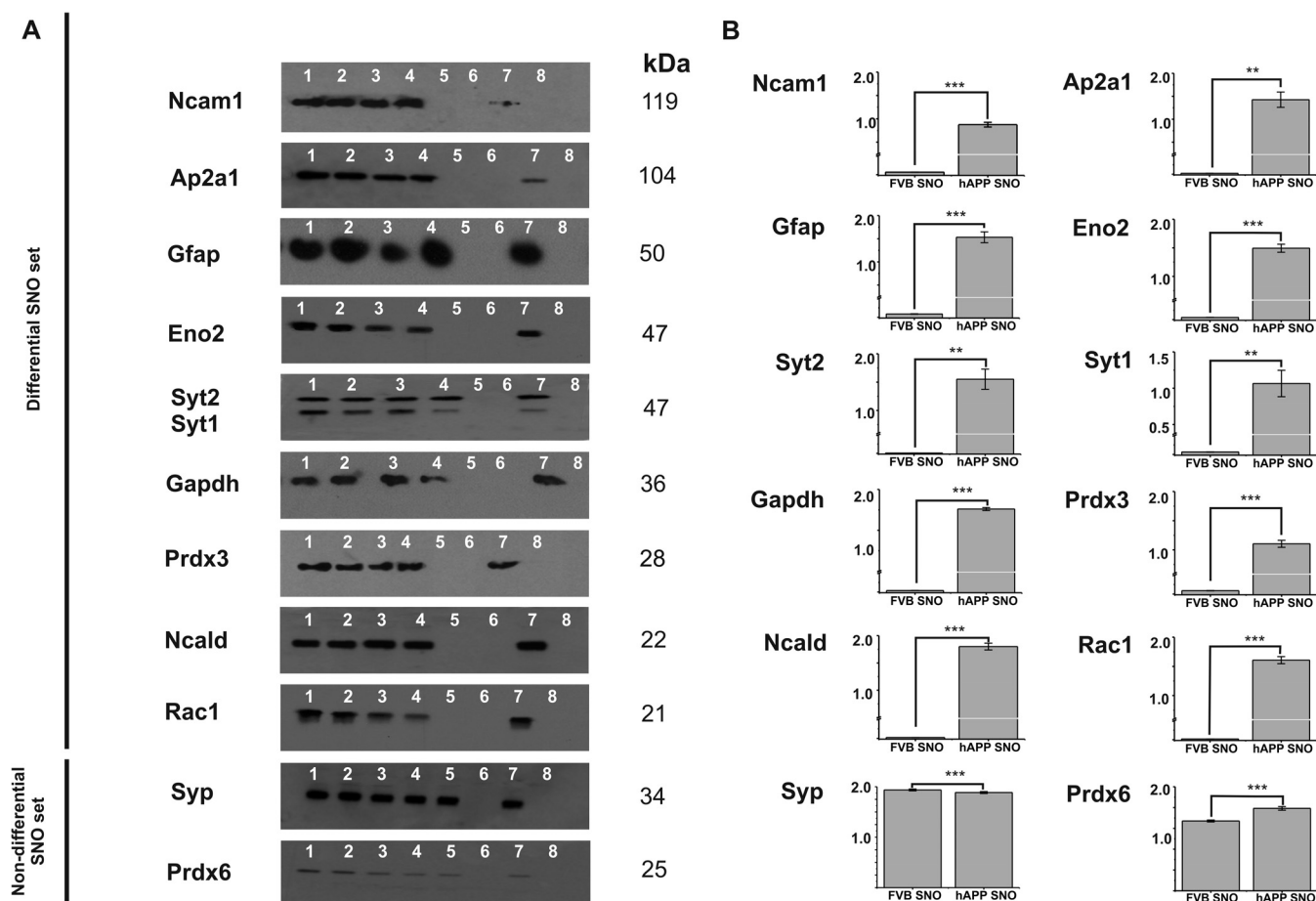
FIG. 7. **Western blot analysis of S-nitrosylated proteins from hAPP brain synaptosomes.** *A*, Synaptosomal SNO-proteins enriched using BST were detected with specific antibodies. Differential SNO set: Ncam1 - Neural cell adhesion molecule, Ap2a1 - AP-2 complex subunit alpha-1, Gfap - Glial fibrillary acidic protein, Eno2 - Gamma enolase, Syt1, Syt2 - Synaptotagmin-1 and 2, Gapdh - glyceraldehyde-3-phosphate dehydrogenase, Ncald - neurocalcin-delta, Prxd3 - peroxiredoxin 3, Rac1- Ras-related C3 botulinum toxin substrate 1 precursor. Non-differential SNO set: Syp- synaptophysin, Prxd6 - peroxiredoxin 6. Lane 1 - total FVB mouse brain lysate, lane 2 - total hAPP brain lysate, lane 3 - soluble fraction (FVB), lane 4 - soluble fraction (hAPP); lane 5 - proteins enriched on neutravidin resin using BST (FVB), lane 6 - neutravidin resin after elution (FVB), lane 7 - proteins enriched on neutravidin resin using BST (hAPP), and lane 8 - neutravidin resin after elution (hAPP). kDa- molecular weight in kilo-Daltons. *B*, Densitometric quantitation of lanes 5 (Neutr_FVB) and 7 (Neutr_hAPP); *n* = 3 experiments, *p* values from *t* test. **-$p \leq 0.01$; ***-$p \leq 0.001$.

cals. Following a number of publications which discussed limitations of BST/SNOSID enrichment methods (96–99), in this work we developed special sample procedures to detect and identify S-nitrosylated proteins in the synapse. We utilized SNOSID enrichment of previously S-nitrosylated tryptic peptides to pinpoint not only the S-nitrosylated proteins but also precise sites of SNO modification. Furthermore, the aim of our study was not to identify the largest number of proteins susceptible to S-nitrosylation in the synapse milieu but rather

to prove that the NO-based regulation is not random that is, related only to higher amount of produced RNS. We also aspired to demonstrate that this process is highly confined to specific key molecules and/or pathways, and is modified upon AD symptoms progression in mice.

By combining an optimized SNOSID method coupled with LC-MS/MS, we identified 138 S-nitrosylated proteins with 249 SNO-sites (Fig. 4) and corresponding changes in pattern of their S-nitrosylation. With this approach 95 SNO-peptides

FIG. 6. *A*, **ClueGO analysis of S-nitrosylated proteins from hAPP mouse brain synaptosomes.** GO biological process/KEGG pathway terms specific for S-nitrosylated proteins from the FVB brain (*-$p \leq 0.05$; **-$p \leq 0.01$). The number of corresponding genes associated with a specific term is indicated as percentage (numbers on bars) and on *x* axis. Ungrouped terms are indicated in yellow. *B*, The networks of functionally grouped terms with nodes linked based on their kappa score ($\geq$0.3). Terms not grouped are shown in yellow. *C*, Interaction network linking human orthologs of differentially SNO-proteins detected in hAPP synaptosomes and Amyloid β precursor protein (APP). The network was sorted according to GO BP criteria. The size of nodes, representing SNO-proteins (in orange) is proportional to the number of SNO-sites, measured in LC-MS/MS experiments. The nodes sharing two most enriched functional terms, axon guidance and cytoplasmic vesicle part are presented as constituents of network modules (represented by dotted spheres).

were identified for the first time, whereas 76% of all identified SNO-proteins were previously described to be endo/exogenously S-nitrosylated in the literature (supplemental Table S2, see literature references). We also observed that almost all SNO-Cys sites in the SNO-diff set (supplemental Table S3) were conserved between human and mouse, suggestive for importance of these sites in the PTM regulation of synaptic functions in the AD brain. An overlap of 25 S-nitrosylated-proteins (Table I and supplemental Table S2) was observed between this study and the one by Zahid *et al.* (92).

To establish the functional connection between identified S-nitrosylated synaptosomal proteins, we applied stringent bioinformatic filtering employing Gene Ontology and pathway data (Figs. 5 and 6). From 100 SNO-proteins identified in wild-type synaptosomes, the majority was linked to various metabolic pathways including: oxidative phosphorylation and energy derivation by oxidation of organic compounds (6 and 24 proteins respectively) and synaptic functions, involving synaptic transmission (18 proteins; Fig. 5 and supplemental Table S4A). The participation of synaptic SNO-proteins in numerous protein classes has been previously described (8, 82). Interestingly, we found for the first time that five proteins linked to synaptic transmission in wild-type synaptosomes (GO:0007268; p = 1.22E-4, supplemental Table S4A) can also be S-nitrosylated (Camk2b, Cplxn1, Kclna2, Nptn, and Synj1). *S*-nitrosylation of both protein kinases and phosphatases influences a wide range of signal transduction pathways mediated by phosphorylation or dephosphorylation (reviewed in (81)). In this view, regulation of Camk2b, Calcium/calmodulin-dependent protein kinase type II beta chain might be important for regulation of synaptic transmission.

To link the changes in S-nitrosylation with advancement of Alzheimer's disease we used a 14 month old transgenic hAPPV717I (hAPP) mouse strain with high neuronal expression of human transgene which recapitulates important pathological and clinical hallmarks of AD, correlated with high burden and accelerated accumulation of Aβ40/42. In order to identify a possibly full spectrum of S-nitrosylation changes we narrowed our investigations to the advanced stage at which mice start to develop Aβ pathology with neuritic plaques (56, 100).

AD patients' brains display elevated level of nitric oxide synthases (70, 71). Moreover, it was found that the iNOS reactivity, expression and calcium-independent enzymatic activity was increased in *APP* transgenic (Tg2576 *APP*) mice and related to cortical neurons and microglial cells (101). Deletion of iNOS in these mice worsened spatial memory, learning, and tau pathology, suggestive for neuroprotective effect of NO (102). Increased levels of iNOS were also detected in cortical neurons stimulated with Aβ peptide (103), and confirmed in functional experiments demonstrating that Aβ stimulated induction of long-term potentiation was inhibited in iNOS knock-out mice (104). Furthermore, treatment with resveratrol protected rats from Aβ-induced neurotoxicity

by suppressing iNOS production (105). Interestingly, in another model of AD (double transgenic *APP-PS1* mice) deletion of iNOS gene alleviated AD-related pathology including increased Aβ levels, plaque formation, gliosis, and premature mortality (103). We confirmed that level of iNOS expression was higher in hAPP synaptosomes as compared with aged-matched controls. Changes in the expression of iNOS and nNOS (Fig. 1) indicate aberrations in the nitric oxide production which may result in subsequent changes of protein S-nitrosylation, observed in hAPP synaptosomes (Fig. 2). Gow *et al.* (106) demonstrated that increased expression of various nitric oxide synthases leads to changes in the level of protein S-nitrosylation in multiple cell types and tissues.

The key factors determining S-nitrosylation sites in proteins are: 1) spatial proximity (*i.e.* complexing with nNOS regulates the S-nitrosylation of NMDARs and PSD-95), 2) presence of signature SNO motifs adjacent to target Cys residue, and 3) local hydrophobicity (*i.e.* closeness to the membrane) (8, 107). Therefore, in parallel to functional clustering analyses we linked the differentially S-nitrosylated proteins from hAPP synaptosomes using network approaches. Interestingly, the majority of SNO-proteins (95%; 36/38 of all) could be linked to APP via one bridging partner resulting in a small network with 59 nodes, when stringent GO BP filtering criteria were applied to multiple interaction data (Fig. 6). Both functional clustering and network approaches revealed that axon guidance term was one of the most enriched functional features shared by differentially S-nitrosylated proteins in hAPP synaptosomes. Axon guidance term was shared by six SNO-proteins of the interaction network (Fig. 6C), including five proteins previously described in literature as possible targets of endo/exogenous S-nitrosylation and one novel, GTPase KRas precursor (Table I). The second enriched functional term, "participation in cytoplasmic vesicle" (GO:004443) was allotted to six SNO-proteins, one of which is a novel S-nitrosylation target, Neurocalcin-delta (Ncald/NCALD). S-nitrosylation of this target has been exclusively confirmed in the hAPP brain, by Western blotting experiments with specific antibodies (Fig. 7). Involvement of APP in axonal guidance and vesicle trafficking was previously described (Fig. 6C; (73, 108–112)). Recent *in silico* analysis of differentially expressed genes in sporadic early onset AD revealed an alteration in biological pathways related to intracellular signaling including axon guidance among the others (113). Moreover, defects in axon guidance were linked to early stage progression of another neurodegenerative disorder, Parkinson's disease (114).

The synaptic cytoskeleton is particularly important for synaptic plasticity and plays a role in rapid activity-dependent changes of synapse volume or shape. Disruptions in the synaptic cytoskeleton affect the stability and maturation of synapses and subsequently disturb neuronal communication (115–117). Actin cytoskeletal pathology may be an early cause of transport defects in AD (118). One of the identified, differentially S-nitrosylated proteins participating in axonal guid-

ance is β-actin (Actb). Actin microfilaments supported by actin-associated proteins, are the dominant cytoskeletal elements structuring synapses. Local β-actin synthesis in developing axons plays an important role in growth cone steering (119). S-nitrosylation of β-actin, which increases formation of short actin filaments lead to alterations in the cytoskeletal network and inhibited dopamine release (120).

Another identified SNO-protein, actin severing protein; cofilin (Cfln) affects APP transport, synaptic stability, and activity (121). siRNA knockdown of cofilin abolished both Aβ and RanBP9-induced apoptosis (122). In hippocampal neurons, fibrillar Aβ was able to alter the PAK1/LIMK1/cofilin axis and thereby actin organization (123).

Rac1, a small Rho GTPase functions as a positive regulator of neurite outgrowth downstream of growth-promoting axon guidance cues. It regulates dendritic spines and excitatory synapses, but little is known about its regulation in synapses (124). Rac1 is related to increased alterations in the actin cytoskeleton induced by fibrillar Aβ (125). It has been hypothesized that Rac1 activation exacerbates AD by shifting actin into a polymerized conformation, a phenomenon observed in various neurodegenerative disorders (125). Previous studies have also shown that the reduction of ROS generation leads to an inhibition of the Rac1 activation (126).

An important group of proteins engaged in the axon guidance are those connected to the endo/exocytosis processes. AP-2 is the major adaptor protein important for sorting of synaptic vesicle proteins during recycling (127). In neurons, AP-2-dependent trafficking of NMDA and AMPA receptors is an essential determinant of synaptic strength and plasticity (128, 129). S-nitrosylation of AMPA receptors resulted in increased endocytosis by binding AP-2 protein (130).

Levels of Neurocalcin, a calcium binding protein identified to be S- nitrosylated for the first time are reduced in AD brain, suggestive for biochemical deficits related to the synaptic degeneration (131). Taken together, the identified changes of S-nitrosylation of proteins linked to axon guidance and related to endo/exocytosis processes underlie an important role of this modification in the regulation of synapses in the AD brain.

Another significantly enriched category of the differentially S-nitrosylated proteins identified in hAPP synaptosomes constituted of those involved in energy metabolism and oxidative phosphorylation (Fig. 6*A*, 6*B* and supplemental Table S5). Modulation of protein function through PTM is probably an important feature of energy production at the synapses. Although the brain represents only 2% of the body weight, it uses ~20% of the total body basal oxygen consumption (132). Previous proteomic analyzes reported significant decrease in level of glycolytic enzymes in the AD brain and increase in the oxidation of proteins involved in the glycolysis and TCA cycle (37, 41).

In the current study, we showed changes in the S-nitrosylation of seven proteins involved in energy metabolism (supplemental Table S5*A*). We, for example, identified aberrant S-nitrosylation of GAPDH a key enzyme in glycolysis process which catalyzes NAD-mediated oxidative phosphorylation of glyceraldehyde phosphate to 1,3-diphosphoglycerate. However, apart from its' classical role in glycolysis, GAPDH takes part in highly diverse, non-glycolytic functions. For example, S-nitrosylation of GAPDH enhances binding to SIAH1 protein, an E3 ubiquitin ligase, and the complex is translocated to nucleus where it activates apoptosis. In the nucleus, SNO-GAPDH not only mediates apoptosis but also serves as a trans-nitrosylase of other nuclear proteins, including SIRT1, HDAC2, or DNAPK (19). SNO-GAPDH dependent molecular pathway leading to neuronal apoptosis may contribute to Alzheimer's disease pathogenesis (76).

A recent study demonstrated that both GAPDH and gamma enolase were oxidatively modified in post mortem AD patients brains (76, 133). Oxidative modifications of these enzymes led to inhibition of glycolytic pathways. This is consistent with the altered glucose tolerance and metabolic changes confirmed in PET analyses of AD patients (134). The impact of S-nitrosylation on the function of those proteins is unclear. Aberrant S-nitrosylation of a large number of glycolytic enzymes suggests that synapses may be sensitive to glycolytic perturbation, which in turn exacerbates Aβ toxicity.

We also found a large group of mitochondrial proteins with altered S-nitrosylation. There is mounting evidence that mitochondrial dysfunction accompanies AD progression and development (135). Mitochondrial dysfunctions are consequences of aberrant redox reactions triggered by high level of NO. Disturbances in the activity of Complexes I and IV caused by S-nitrosylation have been reported in the AD brain (reviewed in (136)). Additionally, a decrease in the activity of F1 ATPAse caused by S-nitrosylation was reported in cardiomyocytes (54). We found that S-nitrosylated Ndufv1/NDUFV1 and Uqcrc1/UQCRC1, mitochondrial complex I and III proteins were either uniquely present (Ndufv1) or more nitrosylated (Uqcrc1/UQCRC1) in APP brains (supplemental Table S2).

Summarizing, these results suggest that altered S-nitrosylation of proteins involved in energy metabolism might be one of the main events associated with AD, leading to reduced activity of metabolic pathways and therefore decreased ATP production, confirming the previous observations.

Cellular "S-nitrosome" homeostasis is regulated by enzymatic and non-enzymatic nitrosylation, denitrosylation, and the overall redox milieu. The current work was based on systematic profiling of S-nitrosylations in brain synaptosomes from wild-type and AD mice. We have identified several endogenous SNO-sites exclusively in the hAPP brain, which further contributes to our understanding of synaptic complexity and its alterations in AD. It also implicates S-nitrosylation in the interplay of various PTM controlling the signaling cascades in the brain, in normal and neurodegenerative conditions, and identifies novel putative drug targets for therapeutic interventions. Further research is necessary to decipher the

precise role of S-nitrosylation in the function of identified synaptic proteins.

REFERENCES

1. Garthwaite, J., Charles, S. L., and Chess-Williams, R. (1988) Endothelium-derived relaxing factor release on activation of NMDA receptors suggests role as intercellular messenger in the brain. *Nature* **336,** 385–388
2. Bredt, D. S., Glatt, C. E., Hwang, P. M., Fotuhi, M., Dawson, T. M., and Snyder, S. H. (1991) Nitric oxide synthase protein and mRNA are discretely localized in neuronal populations of the mammalian CNS together with NADPH diaphorase. *Neuron* **7,** 615–624
3. Dawson, T. M., Bredt, D. S., Fotuhi, M., Hwang, P. M., and Snyder, S. H. (1991) Nitric oxide synthase and neuronal NADPH diaphorase are identical in brain and peripheral tissues. *Proc. Natl. Acad. Sci. U. S. A.* **88,** 7797–7801
4. Drapier, J. C., and Bouton, C. (1996) Modulation by nitric oxide of metalloprotein regulatory activities. *Bioessays* **18,** 549–556
5. Pryor, W. A., and Squadrito, G. L. (1995) The chemistry of peroxynitrite: a product from the reaction of nitric oxide with superoxide. *Am. J. Physiol.* **268,** L699-L722
6. Chiueh, C. C., and Rauhala, P. (1999) The redox pathway of S-nitrosoglutathione, glutathione and nitric oxide in cell to neuron communications. *Free Radic. Res.* **31,** 641–650
7. Lane, P., Hao, G., and Gross, S. S. (2001) S-nitrosylation is emerging as a specific and fundamental posttranslational protein modification: head-to-head comparison with O-phosphorylation. *Sci. STKE* 2001, re1
8. Nakamura, T., Tu, S., Akhtar, M. W., Sunico, C. R., Okamoto, S., and Lipton, S. A. (2013) Aberrant protein s-nitrosylation in neurodegenerative diseases. *Neuron* **78,** 596–614
9. Aranda, E., Lopez-Pedrera, C., De La Haba-Rodriguez, J. R., and Rodriguez-Ariza, A. (2012) Nitric oxide and cancer: the emerging role of S-nitrosylation. *Curr. Mol. Med.* **12,** 50–67
10. Wang, Z. (2012) Protein S-nitrosylation and cancer. *Cancer Lett.* **320,** 123–129
11. Martinez-Ruiz, A., and Lamas, S. (2004) S-nitrosylation: a potential new paradigm in signal transduction. *Cardiovasc. Res.* **62,** 43–52
12. Gonzalez, D. R., Treuer, A., Sun, Q. A., Stamler, J. S., and Hare, J. M. (2009) S-Nitrosylation of cardiac ion channels. *J. Cardiovasc. Pharmacol.* **54,** 188–195
13. Murphy, E., Kohr, M., Sun, J., Nguyen, T., and Steenbergen, C. (2012) S-nitrosylation: a radical way to protect the heart. *J. Mol. Cell Cardiol.* **52,** 568–577
14. Nakamura, T., and Lipton, S. A. (2011) Redox modulation by S-nitrosylation contributes to protein misfolding, mitochondrial dynamics, and neuronal synaptic damage in neurodegenerative diseases. *Cell Death Differ.* **18,** 1478–1486
15. Choi, Y. B., Tenneti, L., Le, D. A., Ortiz, J., Bai, G., Chen, H. S., and Lipton, S. A. (2000) Molecular basis of NMDA receptor-coupled ion channel modulation by S-nitrosylation. *Nat. Neurosci.* **3,** 15–21
16. Nakamura, T., and Lipton, S. A. (2010) Preventing Ca2+-mediated nitrosative stress in neurodegenerative diseases: possible pharmacological strategies. *Cell Calcium* **47,** 190–197
17. Uehara, T., Nakamura, T., Yao, D., Shi, Z. Q., Gu, Z., Ma, Y., Masliah, E., Nomura, Y., and Lipton, S. A. (2006) S-nitrosylated protein-disulfide isomerase links protein misfolding to neurodegeneration. *Nature* **441,** 513–517
18. Nakamura, T., Cieplak, P., Cho, D. H., Godzik, A., and Lipton, S. A. (2010) S-nitrosylation of Drp1 links excessive mitochondrial fission to neuronal injury in neurodegeneration. *Mitochondrion* **10,** 573–578
19. Kornberg, M. D., Sen, N., Hara, M. R., Juluri, K. R., Nguyen, J. V., Snowman, A. M., Law, L., Hester, L. D., and Snyder, S. H. (2010) GAPDH mediates nitrosylation of nuclear proteins. *Nat. Cell Biol.* **12,** 1094–1100
20. Tian, J., Kim, S. F., Hester, L., and Snyder, S. H. (2008) S-nitrosylation/activation of COX-2 mediates NMDA neurotoxicity. *Proc. Natl. Acad. Sci. U. S. A.* **105,** 10537–10540
21. Huang, Y., Man, H. Y., Sekine-Aizawa, Y., Han, Y., Juluri, K., Luo, H., Cheah, J., Lowenstein, C., Huganir, R. L., and Snyder, S. H. (2005) S-nitrosylation of N-ethylmaleimide sensitive factor mediates surface expression of AMPA receptors. *Neuron* **46,** 533–540
22. Sunico, C. R., Nakamura, T., Rockenstein, E., Mante, M., Adame, A., Chan, S. F., Newmeyer, T. F., Masliah, E., Nakanishi, N., and Lipton, S. A. (2013) S-Nitrosylation of parkin as a novel regulator of p53-mediated neuronal cell death in sporadic Parkinson's disease. *Mol. Neurodegener.* **8,** 29
23. Chung, K. K., Thomas, B., Li, X., Pletnikova, O., Troncoso, J. C., Marsh, L., Dawson, V. L., and Dawson, T. M. (2004) S-nitrosylation of parkin regulates ubiquitination and compromises parkin's protective function. *Science* **304,** 1328–1331
24. Ozawa, K., Komatsubara, A. T., Nishimura, Y., Sawada, T., Kawafune, H., Tsumoto, H., Tsuji, Y., Zhao, J., Kyotani, Y., Tanaka, T., Takahashi, R., and Yoshizumi, M. (2013) S-nitrosylation regulates mitochondrial quality control via activation of parkin. *Sci. Rep.* **3,** 2202
25. Sen, N., Hara, M. R., Ahmad, A. S., Cascio, M. B., Kamiya, A., Ehmsen, J. T., Agrawal, N., Aggrawal, N., Hester, L., Dore, S., Snyder, S. H., and Sawa, A. (2009) GOSPEL: a neuroprotective protein that binds to GAPDH upon S-nitrosylation. *Neuron* **63,** 81–91
26. Qu, J., Nakamura, T., Cao, G., Holland, E. A., McKercher, S. R., and Lipton, S. A. (2011) S-Nitrosylation activates Cdk5 and contributes to synaptic spine loss induced by beta-amyloid peptide. *Proc. Natl. Acad. Sci. U. S. A.* **108,** 14330–14335
27. Clementi, E., Brown, G. C., Feelisch, M., and Moncada, S. (1998) Persistent inhibition of cell respiration by nitric oxide: crucial role of S-nitrosylation of mitochondrial complex I and protective action of glutathione. *Proc. Natl. Acad. Sci. U. S. A.* **95,** 7631–7636
28. Selvakumar, B., Huganir, R. L., and Snyder, S. H. (2009) S-nitrosylation of stargazin regulates surface expression of AMPA-glutamate neurotransmitter receptors. *Proc. Natl. Acad. Sci. U. S. A.* **106,** 16440–16445
29. Mustafa, A. K., Kumar, M., Selvakumar, B., Ho, G. P., Ehmsen, J. T., Barrow, R. K., Amzel, L. M., and Snyder, S. H. (2007) Nitric oxide S-nitrosylates serine racemase, mediating feedback inhibition of D-serine formation. *Proc. Natl. Acad. Sci. U. S. A.* **104,** 2950–2955
30. Abbott, A. (2012) Cognition: The brain's decline. *Nature* **492,** S4–S5
31. Komarova, N. L., and Thalhauser, C. J. (2011) High degree of heterogeneity in Alzheimer's disease progression patterns. *PLoS Comput. Biol.* **7,** e1002251
32. da Cruz e Silva, O. A., Henriques, A. G., Domingues, S. C., and da Cruz e Silva, E. F. (2010) Wnt signalling is a relevant pathway contributing to amyloid beta- peptide-mediated neuropathology in Alzheimer's disease. *CNS Neurol. Disord. Drug Targets* **9,** 720–726
33. Liu, Y., Liu, F., Grundke-Iqbal, I., Iqbal, K., and Gong, C. X. (2011) Deficient brain insulin signalling pathway in Alzheimer's disease and diabetes. *J. Pathol.* **225,** 54–62
34. Munoz, L., and Ammit, A. J. (2010) Targeting p38 MAPK pathway for the treatment of Alzheimer's disease. *Neuropharmacology* **58,** 561–568

35. Silvestrelli, G., Lanari, A., Parnetti, L., Tomassoni, D., and Amenta, F. (2006) Treatment of Alzheimer's disease: from pharmacology to a better understanding of disease pathophysiology. *Mech. Ageing Dev.* **127,** 148–157

36. Agostinho, P., Cunha, R. A., and Oliveira, C. (2010) Neuroinflammation, oxidative stress, and the pathogenesis of Alzheimer's disease. *Curr. Pharm. Des.* **16,** 2766–2778

37. Sultana, R., and Butterfield, D. A. (2010) Role of oxidative stress in the progression of Alzheimer's disease. *J. Alzheimers Dis.* **19,** 341–353

38. Malinski, T. (2007) Nitric oxide and nitroxidative stress in Alzheimer's disease. *J. Alzheimers Dis.* **11,** 207–218

39. Aluise, C. D., Robinson, R. A., Cai, J., Pierce, W. M., Markesbery, W. R., and Butterfield, D. A. (2011) Redox proteomics analysis of brains from subjects with amnestic mild cognitive impairment compared to brains from subjects with preclinical Alzheimer's disease: insights into memory loss in MCI. *J. Alzheimers Dis.* **23,** 257–269

40. Barone, E., Di Domenico, F., Cenini, G., Sultana, R., Coccia, R., Preziosi, P., Perluigi, M., Mancuso, C., and Butterfield, D. A. (2011) Oxidative and nitrosative modifications of biliverdin reductase-A in the brain of subjects with Alzheimer's disease and amnestic mild cognitive impairment. *J. Alzheimers Dis.* **25,** 623–633

41. Butterfield, D. A., and Sultana, R. (2007) Redox proteomics identification of oxidatively modified brain proteins in Alzheimer's disease and mild cognitive impairment: insights into the progression of this dementing disorder. *J. Alzheimers Dis.* **12,** 61–72

42. Robinson, R. A., Lange, M. B., Sultana, R., Galvan, V., Fombonne, J., Gorostiza, O., Zhang, J., Warrier, G., Cai, J., Pierce, W. M., Bredesen, D. E., and Butterfield, D. A. (2011) Differential expression and redox proteomics analyses of an Alzheimer disease transgenic mouse model: effects of the amyloid-beta peptide of amyloid precursor protein. *Neuroscience* **177,** 207–222

43. Sultana, R., Robinson, R. A., Di Domenico, F., Abdul, H. M., St Clair, D. K., Markesbery, W. R., Cai, J., Pierce, W. M., and Butterfield, D. A. (2011) Proteomic identification of specifically carbonylated brain proteins in APP(NLh)/APP(NLh) x PS-1(P264L)/PS-1(P264L) human double mutant knock-in mouse model of Alzheimer disease as a function of age. *J. Proteomics* **74,** 2430–2440

44. Finkel, T. (2011) Signal transduction by reactive oxygen species. *J. Cell Biol.* **194,** 7–15

45. Fransen, M., Nordgren, M., Wang, B., and Apanasets, O. (2012) Role of peroxisomes in ROS/RNS-metabolism: implications for human disease. *Biochim. Biophys. Acta* **1822,** 1363–1373

46. Valko, M., Leibfritz, D., Moncol, J., Cronin, M. T., Mazur, M., and Telser, J. (2007) Free radicals and antioxidants in normal physiological functions and human disease. *Int. J. Biochem. Cell Biol.* **39,** 44–84

47. Westerblad, H., and Allen, D. G. (2011) Emerging roles of ROS/RNS in muscle function and fatigue. *Antioxid. Redox Signal* **15,** 2487–2499

48. Games, D., Buttini, M., Kobayashi, D., Schenk, D., and Seubert, P. (2006) Mice as models: transgenic approaches and Alzheimer's disease. *J. Alzheimers Dis.* **9,** 133–149

49. Marchetti, C., and Marie, H. (2011) Hippocampal synaptic plasticity in Alzheimer's disease: what have we learned so far from transgenic models? *Rev. Neurosci.* **22,** 373–402

50. Hao, G., Derakhshan, B., Shi, L., Campagne, F., and Gross, S. S. (2006) SNOSID, a proteomic method for identification of cysteine S-nitrosylation sites in complex protein mixtures. *Proc. Natl. Acad. Sci. U. S. A.* **103,** 1012–1017

51. Jaffrey, S. R., and Snyder, S. H. (2001) The biotin switch method for the detection of S-nitrosylated proteins. *Sci. STKE* 2001, pl1

52. Martinez-Ruiz, A., and Lamas, S. (2004) Detection and proteomic identification of S-nitrosylated proteins in endothelial cells. *Arch. Biochem. Biophys.* **423,** 192–199

53. Ohtake, K., Shimada, N., Uchida, H., and Kobayashi, J. (2009) Proteomic approach for identification of protein S-nitrosation in mouse gastric mucosa treated with S-nitrosoglutathione. *J. Proteomics* **72,** 750–760

54. Sun, J., Morgan, M., Shen, R. F., Steenbergen, C., and Murphy, E. (2007) Preconditioning results in S-nitrosylation of proteins involved in regulation of mitochondrial energetics and calcium transport. *Circ. Res.* **101,** 1155–1163

55. Tannenbaum, S. R., and White, F. M. (2006) Regulation and specificity of S-nitrosylation and denitrosylation. *ACS Chem. Biol.* **1,** 615–618

56. Moechars, D., Dewachter, I., Lorent, K., Reverse, D., Baekelandt, V., Naidu, A., Tesseur, I., Spittaels, K., Haute, C. V., Checler, F., Godaux, E., Cordell, B., and Van Leuven, F. (1999) Early phenotypic changes in transgenic mice that overexpress different mutants of amyloid precursor protein in brain. *J. Biol. Chem.* **274,** 6483–6492

57. Linetska, M. V., Storchak, L. G., Tarasenko, A. S., and Himmelreich, N. H. (2004) Involvement of membrane GABA transporter in alpha-latrotoxin-stimulated [3H]GABA release. *Neurochem. Int.* **44,** 303–312

58. Tarasenko, A. S., Kostrzhevska, O. G., Storchak, L. G., Linetska, M. V., Borisova, T. A., and Himmelreich, N. H. (2005) Phenylarsine oxide is able to dissipate synaptic vesicle acidic pool. *Neurochem. Int.* **46,** 541–550

59. Bakun, M., Karczmarski, J., Poznanski, J., Rubel, T., Rozga, M., Malinowska, A., Sands, D., Hennig, E., Oledzki, J., Ostrowski, J., and Dadlez, M. (2009) An integrated LC-ESI-MS platform for quantitation of serum peptide ladders. Application for colon carcinoma study. *Proteomics Clin. Appl* **3,** 932–946

60. Sikora, J., Towpik, J., Graczyk, D., Kistowski, M., Rubel, T., Poznanski, J., Langridge, J., Hughes, C., Dadlez, M., and Boguta, M. (2009) Yeast prion [PSI+] lowers the levels of mitochondrial prohibitins. *Biochim. Biophys. Acta* **1793,** 1703–1709

61. Bakun, M., Niemczyk, M., Domanski, D., Jazwiec, R., Perzanowska, A., Niemczyk, S., Kistowski, M., Fabijanska, A., Borowiec, A., Paczek, L., and Dadlez, M. (2012) Urine proteome of autosomal dominant polycystic kidney disease patients. *Clin. Proteomics* **9,** 13

62. Mikula, M., Gaj, P., Dzwonek, K., Rubel, T., Karczmarski, J., Paziewska, A., Dzwonek, A., Bragoszewski, P., Dadlez, M., and Ostrowski, J. (2010) Comprehensive analysis of the palindromic motif TCTCGCGAGA: a regulatory element of the HNRNPK promoter. *DNA Res.* **17,** 245–260

63. Orlowska, K. P., Klosowska, K., Szczesny, R. J., Cysewski, D., Krawczyk, P. S., and Dziembowski, A. (2013) A new strategy for gene targeting and functional proteomics using the DT40 cell line. *Nucleic Acids Res.* **41,** e167

64. Oliveros, J. C. (2007) VENNY. An interactive tool for comparing lists with Venn Diagrams. http://bioinfogp.cnb.csic.es/tools/venny/index.html.

65. Warde-Farley, D., Donaldson, S. L., Comes, O., Zuberi, K., Badrawi, R., Chao, P., Franz, M., Grouios, C., Kazi, F., Lopes, C. T., Maitland, A., Mostafavi, S., Montojo, J., Shao, Q., Wright, G., Bader, G. D., and Morris, Q. (2010) The GeneMANIA prediction server: biological network integration for gene prioritization and predicting gene function. *Nucleic Acids Res.* **38,** W214–W220

66. Zuberi, K., Franz, M., Rodriguez, H., Montojo, J., Lopes, C. T., Bader, G. D., and Morris, Q. (2013) GeneMANIA prediction server 2013 update. *Nucleic Acids Res.* **41,** W115–W122

67. Bindea, G., Mlecnik, B., Hackl, H., Charoentong, P., Tosolini, M., Kirilovsky, A., Fridman, W. H., Pages, F., Trajanoski, Z., and Galon, J. (2009) ClueGO: a Cytoscape plug-in to decipher functionally grouped gene ontology and pathway annotation networks. *Bioinformatics* **25,** 1091–1093

68. von Eichborn, J., Dunkel, M., Gohlke, B. O., Preissner, S. C., Hoffmann, M. F., Bauer, J. M., Armstrong, J. D., Schaefer, M. H., Andrade-Navarro, M. A., Le Novere, N., Croning, M. D., Grant, S. G., van Nierop, P., Smit, A. B., and Preissner, R. (2013) SynSysNet: integration of experimental data on synaptic protein-protein interactions with drug-target relations. *Nucleic Acids Res.* **41,** D834–D840

69. Pirooznia, M., Wang, T., Avramopoulos, D., Valle, D., Thomas, G., Huganir, R. L., Goes, F. S., Potash, J. B., and Zandi, P. P. (2012) SynaptomeDB: an ontology-based knowledgebase for synaptic genes. *Bioinformatics* **28,** 897–899

70. Luth, H. J., Holzer, M., Gartner, U., Staufenbiel, M., and Arendt, T. (2001) Expression of endothelial and inducible NOS-isoforms is increased in Alzheimer's disease, in APP23 transgenic mice and after experimental brain lesion in rat: evidence for an induction by amyloid pathology. *Brain Res.* **913,** 57–67

71. Fernandez-Vizarra, P., Fernandez, A. P., Castro-Blanco, S., Encinas, J. M., Serrano, J., Bentura, M. L., Munoz, P., Martinez-Murillo, R., and Rodrigo, J. (2004) Expression of nitric oxide system in clinically evaluated cases of Alzheimer's disease. *Neurobiol. Dis.* **15,** 287–305

72. Vella, L. J., Sharples, R. A., Nisbet, R. M., Cappai, R., and Hill, A. F. (2008) The role of exosomes in the processing of proteins associated with neurodegenerative diseases. *Eur. Biophys. J* **37,** 323–332

73. Groemer, T. W., Thiel, C. S., Holt, M., Riedel, D., Hua, Y., Huve, J., Wilhelm, B. G., and Klingauf, J. (2011) Amyloid precursor protein is trafficked and secreted via synaptic vesicles. *PLoS One* **6,** e18754

74. Cottrell, B. A., Galvan, V., Banwait, S., Gorostiza, O., Lombardo, C. R., Williams, T., Schilling, B., Peel, A., Gibson, B., Koo, E. H., Link, C. D., and Bredesen, D. E. (2005) A pilot proteomic study of amyloid precursor interactors in Alzheimer's disease. *Ann. Neurol.* **58,** 277–289

75. Aisa, B., Gil-Bea, F. J., Solas, M., Garcia-Alloza, M., Chen, C. P., Lai, M. K., Francis, P. T., and Ramirez, M. J. (2010) Altered NCAM expression associated with the cholinergic system in Alzheimer's disease. *J. Alzheimers Dis.* **20,** 659–668

76. Butterfield, D. A., Hardas, S. S., and Lange, M. L. (2010) Oxidatively modified glyceraldehyde-3-phosphate dehydrogenase (GAPDH) and Alzheimer's disease: many pathways to neurodegeneration. *J. Alzheimers Dis.* **20,** 369–393

77. Kim, S. H., Fountoulakis, M., Cairns, N., and Lubec, G. (2001) Protein levels of human peroxiredoxin subtypes in brains of patients with Alzheimer's disease and Down syndrome. *J. Neural Transm. Suppl*, 223–235

78. Krapfenbauer, K., Engidawork, E., Cairns, N., Fountoulakis, M., and Lubec, G. (2003) Aberrant expression of peroxiredoxin subtypes in neurodegenerative disorders. *Brain Res.* **967,** 152–160

79. Rudinskiy, N., Grishchuk, Y., Vaslin, A., Puyal, J., Delacourte, A., Hirling, H., Clarke, P. G., and Luthi-Carter, R. (2009) Calpain hydrolysis of alpha- and beta2-adaptins decreases clathrin-dependent endocytosis and may promote neurodegeneration. *J. Biol. Chem.* **284,** 12447–12458

80. Calabrese, V., Cornelius, C., Rizzarelli, E., Owen, J. B., Dinkova-Kostova, A. T., and Butterfield, D. A. (2009) Nitric oxide in cell survival: a janus molecule. *Antioxid. Redox Signal* **11,** 2717–2739

81. Hess, D. T., and Stamler, J. S. (2012) Regulation by S-nitrosylation of protein post-translational modification. *J. Biol. Chem.* **287,** 4411–4418

82. Seth, D., and Stamler, J. S. (2011) The SNO-proteome: causation and classifications. *Curr. Opin. Chem. Biol.* **15,** 129–136

83. Jeon, G. S., Nakamura, T., Lee, J. S., Choi, W. J., Ahn, S. W., Lee, K. W., Sung, J. J., and Lipton, S. A. (2014) Potential effect of S-Nitrosylated protein disulfide isomerase on Mutant SOD1 aggregation and neuronal cell death in amyotrophic lateral sclerosis. *Mol. Neurobiol.* **49,** 796–807

84. Walker, A. K., Farg, M. A., Bye, C. R., McLean, C. A., Horne, M. K., and Atkin, J. D. (2010) Protein disulphide isomerase protects against protein aggregation and is S-nitrosylated in amyotrophic lateral sclerosis. *Brain* **133,** 105–116

85. Haun, F., Nakamura, T., Shiu, A. D., Cho, D. H., Tsunemi, T., Holland, E. A., La Spada, A. R., and Lipton, S. A. (2013) S-Nitrosylation of dynamin-related protein 1 mediates mutant huntingtin-induced mitochondrial fragmentation and neuronal injury in huntington's disease. *Antioxid. Redox Signal* **19,** 1173–1184

86. Bai, F., and Witzmann, F. A. (2007) Synaptosome proteomics. *Subcell Biochem.* **43,** 77–98

87. Morciano, M., Beckhaus, T., Karas, M., Zimmermann, H., and Volknandt, W. (2009) The proteome of the presynaptic active zone: from docked synaptic vesicles to adhesion molecules and maxi-channels. *J. Neurochem.* **108,** 662–675

88. Raiteri, L., and Raiteri, M. (2000) Synaptosomes still viable after 25 years of superfusion. *Neurochem. Res.* **25,** 1265–1274

89. Martinez-Ruiz, A., Araujo, I. M., Izquierdo-Alvarez, A., Hernansanz-Agustin, P., Lamas, S., and Serrador, J. M. (2013) Specificity in S-Nitrosylation: A Short-Range Mechanism for NO Signaling? *Antioxid. Redox Signal* **19,** 1220–1235

90. Banerjee, S., Liao, L., Russo, R., Nakamura, T., McKercher, S. R., Okamoto, S., Haun, F., Nikzad, R., Zaidi, R., Holland, E., Eroshkin, A., Yates, J. R., 3rd, and Lipton, S. A. (2012) Isobaric tagging-based quantification by mass spectrometry of differentially regulated proteins in synaptosomes of HIV/gp120 transgenic mice: implications for HIV-associated neurodegeneration. *Exp. Neurol.* **236,** 298–306

91. Koch, S., Scifo, E., Rokka, A., Trippner, P., Lindfors, M., Korhonen, R., Corthals, G. L., Virtanen, I., Lalowski, M., and Tyynela, J. (2013) Cathepsin D deficiency induces cytoskeletal changes and affects cell migration pathways in the brain. *Neurobiol. Dis.* **50,** 107–119

92. Zahid, S., Khan, R., Oellerich, M., Ahmed, N., and Asif, A. R. (2014) Differential S-nitrosylation of proteins in Alzheimer's disease. *Neuroscience* **256,** 126–136

93. Schmitt, F. A., Nelson, P. T., Abner, E., Scheff, S., Jicha, G. A., Smith, C., Cooper, G., Mendiondo, M., Danner, D. D., Van Eldik, L. J., Caban-Holt, A., Lovell, M. A., and Kryscio, R. J. (2012) University of Kentucky Sanders-Brown healthy brain aging volunteers: donor characteristics, procedures, and neuropathology. *Curr. Alzheimer Res.* **9,** 724–733

94. Daiber, A., Daub, S., Bachschmid, M., Schildknecht, S., Oelze, M., Steven, S., Schmidt, P., Megner, A., Wada, M., Tanabe, T., Munzel, T., Bottari, S., and Ullrich, V. (2013) Protein tyrosine nitration and thiol oxidation by peroxynitrite-strategies to prevent these oxidative modifications. *Int. J. Mol. Sci.* **14,** 7542–7570

95. Cho, D. H., Nakamura, T., Fang, J., Cieplak, P., Godzik, A., Gu, Z., and Lipton, S. A. (2009) S-nitrosylation of Drp1 mediates beta-amyloid-related mitochondrial fission and neuronal injury. *Science* **324,** 102–105

96. Forrester, M. T., Foster, M. W., Benhar, M., and Stamler, J. S. (2009) Detection of protein S-nitrosylation with the biotin-switch technique. *Free Radic. Biol. Med.* **46,** 119–126

97. Forrester, M. T., Foster, M. W., and Stamler, J. S. (2007) Assessment and application of the biotin switch technique for examining protein S-nitrosylation under conditions of pharmacologically induced oxidative stress. *J. Biol. Chem.* **282,** 13977–13983

98. Raju, K., Doulias, P. T., Tenopoulou, M., Greene, J. L., and Ischiropoulos, H. (2012) Strategies and tools to explore protein S-nitrosylation. *Biochim. Biophys. Acta* **1820,** 684–688

99. Torta, F., Usuelli, V., Malgaroli, A., and Bachi, A. (2008) Proteomic analysis of protein S-nitrosylation. *Proteomics* **8,** 4484–4494

100. Dewachter, I., van Dorpe, J., Spittaels, K., Tesseur, I., Van Den Haute, C., Moechars, D., and Van Leuven, F. (2000) Modeling Alzheimer's disease in transgenic mice: effect of age and of presenilin1 on amyloid biochemistry and pathology in APP/London mice. *Exp. Gerontol.* **35,** 831–841

101. Rodrigo, J., Fernandez-Vizarra, P., Castro-Blanco, S., Bentura, M. L., Nieto, M., Gomez-Isla, T., Martinez-Murillo, R., Martlnez, A., Serrano, J., and Fernandez, A. P. (2004) Nitric oxide in the cerebral cortex of amyloid-precursor protein (SW) Tg2576 transgenic mice. *Neuroscience* **128,** 73–89

102. Wilcock, D. M., Lewis, M. R., Van Nostrand, W. E., Davis, J., Previti, M. L., Gharkholonarehe, N., Vitek, M. P., and Colton, C. A. (2008) Progression of amyloid pathology to Alzheimer's disease pathology in an amyloid precursor protein transgenic mouse model by removal of nitric oxide synthase 2. *J. Neurosci.* **28,** 1537–1545

103. Nathan, C., Calingasan, N., Nezezon, J., Ding, A., Lucia, M. S., La Perle, K., Fuortes, M., Lin, M., Ehrt, S., Kwon, N. S., Chen, J., Vodovotz, Y., Kipiani, K., and Beal, M. F. (2005) Protection from Alzheimer's-like disease in the mouse by genetic ablation of inducible nitric oxide synthase. *J. Exp. Med.* **202,** 1163–1169

104. Wang, Q., Rowan, M. J., and Anwyl, R. (2004) Beta-amyloid-mediated inhibition of NMDA receptor-dependent long-term potentiation induction involves activation of microglia and stimulation of inducible nitric oxide synthase and superoxide. *J. Neurosci.* **24,** 6049–6056

105. Huang, T. C., Lu, K. T., Wo, Y. Y., Wu, Y. J., and Yang, Y. L. (2011) Resveratrol protects rats from Abeta-induced neurotoxicity by the reduction of iNOS expression and lipid peroxidation. *PLoS One* **6,** e29102

106. Gow, A. J., Chen, Q., Hess, D. T., Day, B. J., Ischiropoulos, H., and Stamler, J. S. (2002) Basal and stimulated protein S-nitrosylation in multiple cell types and tissues. *J. Biol. Chem.* **277,** 9637–9640

107. Kohr, M. J., Aponte, A. M., Sun, J., Wang, G., Murphy, E., Gucek, M., and Steenbergen, C. (2011) Characterization of potential S-nitrosylation sites in the myocardium. *Am. J. Physiol. Heart Circ. Physiol.* **300,** H1327–H1335

108. Chivet, M., Javalet, C., Hemming, F., Pernet-Gallay, K., Laulagnier, K., Fraboulet, S., and Sadoul, R. (2013) Exosomes as a novel way of interneuronal communication. *Biochem. Soc. Trans.* **41,** 241–244

109. Kins, S., Lauther, N., Szodorai, A., and Beyreuther, K. (2006) Subcellular trafficking of the amyloid precursor protein gene family and its pathogenic role in Alzheimer's disease. *Neurodegener. Dis.* **3,** 218–226

110. Magdesian, M. H., Gralle, M., Guerreiro, L. H., Beltrao, P. J., Carvalho, M. M., Santos, L. E., de Mello, F. G., Reis, R. A., and Ferreira, S. T. (2011) Secreted human amyloid precursor protein binds semaphorin 3a and prevents semaphorin-induced growth cone collapse. *PLoS One* **6,** e22857

111. Mizumaru, C., Saito, Y., Ishikawa, T., Yoshida, T., Yamamoto, T., Nakaya, T., and Suzuki, T. (2009) Suppression of APP-containing vesicle traf-

ficking and production of beta-amyloid by AID/DHHC-12 protein. *J. Neurochem.* **111,** 1213–1224

112. Sosa, L. J., Bergman, J., Estrada-Bernal, A., Glorioso, T. J., Kittelson, J. M., and Pfenninger, K. H. (2013) Amyloid precursor protein is an autonomous growth cone adhesion molecule engaged in contact guidance. *PLoS One* **8,** e64521

113. Antonell, A., Llado, A., Altirriba, J., Botta-Orfila, T., Balasa, M., Fernandez, M., Ferrer, I., Sanchez-Valle, R., and Molinuevo, J. L. (2013) A preliminary study of the whole-genome expression profile of sporadic and monogenic early-onset Alzheimer's disease. *Neurobiol. Aging* **34,** 1772–1778

114. Lin, L., Lesnick, T. G., Maraganore, D. M., and Isacson, O. (2009) Axon guidance and synaptic maintenance: preclinical markers for neurodegenerative disease and therapeutics. *Trends Neurosci.* **32,** 142–149

115. De Vos, K. J., Grierson, A. J., Ackerley, S., and Miller, C. C. (2008) Role of axonal transport in neurodegenerative diseases. *Annu. Rev. Neurosci.* **31,** 151–173

116. Lazarov, O., Morfini, G. A., Pigino, G., Gadadhar, A., Chen, X., Robinson, J., Ho, H., Brady, S. T., and Sisodia, S. S. (2007) Impairments in fast axonal transport and motor neuron deficits in transgenic mice expressing familial Alzheimer's disease-linked mutant presenilin 1. *J. Neurosci.* **27,** 7011–7020

117. Stokin, G. B., Lillo, C., Falzone, T. L., Brusch, R. G., Rockenstein, E., Mount, S. L., Raman, R., Davies, P., Masliah, E., Williams, D. S., and Goldstein, L. S. (2005) Axonopathy and transport deficits early in the pathogenesis of Alzheimer's disease. *Science* **307,** 1282–1288

118. Penzes, P., and Vanleeuwen, J. E. (2011) Impaired regulation of synaptic actin cytoskeleton in Alzheimer's disease. *Brain Res. Rev.* **67,** 184–192

119. Welshhans, K., and Bassell, G. J. (2011) Netrin-1-induced local beta-actin synthesis and growth cone guidance requires zipcode binding protein 1. *J. Neurosci.* **31,** 9800–9813

120. Lu, J., Katano, T., Okuda-Ashitaka, E., Oishi, Y., Urade, Y., and Ito, S. (2009) Involvement of S-nitrosylation of actin in inhibition of neurotransmitter release by nitric oxide. *Mol. Pain* **5,** 58

121. Maloney, M. T., and Bamburg, J. R. (2007) Cofilin-mediated neurodegeneration in Alzheimer's disease and other amyloidopathies. *Mol. Neurobiol.* **35,** 21–44

122. Woo, J. A., Jung, A. R., Lakshmana, M. K., Bedrossian, A., Lim, Y., Bu, J. H., Park, S. A., Koo, E. H., Mook-Jung, I., and Kang, D. E. (2012) Pivotal role of the RanBP9-cofilin pathway in Abeta-induced apoptosis and neurodegeneration. *Cell Death Differ.* **19,** 1413–1423

123. Mendoza-Naranjo, A., Contreras-Vallejos, E., Henriquez, D. R., Otth, C., Bamburg, J. R., Maccioni, R. B., and Gonzalez-Billault, C. (2012) Fibrillar amyloid-beta1–42 modifies actin organization affecting the cofilin phosphorylation state: a role for Rac1/cdc42 effector proteins and the slingshot phosphatase. *J. Alzheimers Dis.* **29,** 63–77

124. Oh, D., Han, S., Seo, J., Lee, J. R., Choi, J., Groffen, J., Kim, K., Cho, Y. S., Choi, H. S., Shin, H., Woo, J., Won, H., Park, S. K., Kim, S. Y., Jo, J., Whitcomb, D. J., Cho, K., Kim, H., Bae, Y. C., Heisterkamp, N., Choi, S. Y., and Kim, E. (2010) Regulation of synaptic Rac1 activity, long-term potentiation maintenance, and learning, and memory by BCR and ABR Rac GTPase-activating proteins. *J. Neurosci.* **30,** 14134–14144

125. Mendoza-Naranjo, A., Gonzalez-Billault, C., and Maccioni, R. B. (2007) Abeta1–42 stimulates actin polymerization in hippocampal neurons through Rac1 and Cdc42 Rho GTPases. *J. Cell Sci.* **120,** 279–288

126. Nozoe, M., Hirooka, Y., Koga, Y., Sagara, Y., Kishi, T., Engelhardt, J. F., and Sunagawa, K. (2007) Inhibition of Rac1-derived reactive oxygen species in nucleus tractus solitarius decreases blood pressure and heart rate in stroke-prone spontaneously hypertensive rats. *Hypertension* **50,** 62–68

127. Traub, L. M. (2009) Tickets to ride: selecting cargo for clathrin-regulated internalization. *Nat. Rev. Mol. Cell Biol.* **10,** 583–596

128. Kastning, K., Kukhtina, V., Kittler, J. T., Chen, G., Pechstein, A., Enders, S., Lee, S. H., Sheng, M., Yan, Z., and Haucke, V. (2007) Molecular determinants for the interaction between AMPA receptors and the clathrin adaptor complex AP-2. *Proc. Natl. Acad. Sci. U. S. A.* **104,** 2991–2996

129. Lavezzari, G., McCallum, J., Lee, R., and Roche, K. W. (2003) Differential binding of the AP-2 adaptor complex and PSD-95 to the C-terminus of the NMDA receptor subunit NR2B regulates surface expression. *Neuropharmacology* **45,** 729–737

130. Selvakumar, B., Jenkins, M. A., Hussain, N. K., Huganir, R. L., Traynelis, S. F., and Snyder, S. H. (2013) S-nitrosylation of AMPA receptor GluA1 regulates phosphorylation, single-channel conductance, and endocytosis. *Proc. Natl. Acad. Sci. U. S. A.* **110,** 1077–1082

131. Shimohama, S., Chachin, M., Taniguchi, T., Hidaka, H., and Kimura, J. (1996) Changes of neurocalcin, a calcium-binding protein, in the brain of patients with Alzheimer's disease. *Brain Res.* **716,** 233–236

132. Mink, J. W., Blumenschine, R. J., and Adams, D. B. (1981) Ratio of central nervous system to body metabolism in vertebrates: its constancy and functional basis. *Am. J. Physiol.* **241,** R203–R212

133. Butterfield, D. A., and Lange, M. L. (2009) Multifunctional roles of enolase in Alzheimer's disease brain: beyond altered glucose metabolism. *J. Neurochem.* **111,** 915–933

134. Kuntzelmann, A., Guenther, T., Haberkorn, U., Essig, M., Giesel, F., Henze, R., Schroeter, M. L., Schroder, J., and Schonknecht, P. (2013) Impaired cerebral glucose metabolism in prodromal Alzheimer's disease differs by regional intensity normalization. *Neurosci. Lett.* **534,** 12–17

135. Swerdlow, R. H., Burns, J. M., and Khan, S. M. (2013) The Alzheimer's disease mitochondrial cascade hypothesis: progress and perspectives. *Biochim. Biophys. Acta*

136. Nakamura, T., and Lipton, S. A. (2013) Emerging role of protein-protein transnitrosylation in cell signaling pathways. *Antioxid. Redox Signal* **18,** 239–249

137. Riederer, I. M., Schiffrin, M., Kovari, E., Bouras, C., and Riederer, B. M. (2009) Ubiquitination and cysteine nitrosylation during aging and Alzheimer's disease. *Brain Res. Bull.* **80,** 233–241

138. Doulias, P. T., Greene, J. L., Greco, T. M., Tenopoulou, M., Seeholzer, S. H., Dunbrack, R. L., and Ischiropoulos, H. (2010) Structural profiling of endogenous S-nitrosocysteine residues reveals unique features that accommodate diverse mechanisms for protein S-nitrosylation. *Proc. Natl. Acad. Sci. U. S. A.* **107,** 16958–16963

139. Huang, B., and Chen, C. (2010) Detection of protein S-nitrosation using irreversible biotinylation procedures (IBP). *Free Radic. Biol. Med.* **49,** 447–456

140. Tello, D., Tarin, C., Ahicart, P., Breton-Romero, R., Lamas, S., and Martinez-Ruiz, A. (2009) A "fluorescence switch" technique increases the sensitivity of proteomic detection and identification of S-nitrosylated proteins. *Proteomics* **9,** 5359–5370

141. Paige, J. S., Xu, G., Stancevic, B., and Jaffrey, S. R. (2008) Nitrosothiol reactivity profiling identifies S-nitrosylated proteins with unexpected stability. *Chem. Biol.* **15,** 1307–1316

142. Liu, M., Hou, J., Huang, L., Huang, X., Heibeck, T. H., Zhao, R., Pasa-Tolic, L., Smith, R. D., Li, Y., Fu, K., Zhang, Z., Hinrichs, S. H., and Ding, S. J. (2010) Site-specific proteomics approach for study protein S-nitrosylation. *Anal. Chem.* **82,** 7160–7168

143. Gao, C., Guo, H., Wei, J., Mi, Z., Wai, P. Y., and Kuo, P. C. (2005) Identification of S-nitrosylated proteins in endotoxin-stimulated RAW264.7 murine macrophages. *Nitric Oxide* **12,** 121–126

144. Forrester, M. T., Thompson, J. W., Foster, M. W., Nogueira, L., Moseley, M. A., and Stamler, J. S. (2009) Proteomic analysis of S-nitrosylation and denitrosylation by resin-assisted capture. *Nat. Biotechnol.* **27,** 557–559

145. Doulias, P. T., Tenopoulou, M., Greene, J. L., Raju, K., and Ischiropoulos, H. (2013) Nitric oxide regulates mitochondrial fatty acid metabolism through reversible protein S-nitrosylation. *Sci. Signal.* **6,** rs1